

Reflective Cracking Study: First-level Report on HVS Testing on Section 588RF — 90 mm AR4000-D Overlay

Authors:
D. Jones, R. Wu and J. Harvey

Partnered Pavement Research Program (PPRC) Contract Strategic Plan Element 4.10:
Development of Improved Rehabilitation Designs for Reflective Cracking

PREPARED FOR:

California Department of Transportation
Division of Research and Innovation
Office of Roadway Research

PREPARED BY:

University of California
Pavement Research Center
UC Davis, UC Berkeley



Title: Reflective Cracking Study: First-level Report on HVS Testing on Section 588RF - 90 mm AR4000-D Overlay

Authors: D. Jones, R. Wu and J. Harvey

Prepared for:
Caltrans

FHWA No:
CA091073D

Date:
August 2006

Contract No:
65A0172

Client Reference No:
SPE 4.10

Status:
Stage 6, Approved Version

Abstract:

This report is the fourth in a series of first-level analysis reports that describe the results of HVS testing on a full-scale experiment being performed at the Richmond Field Station (RFS) to validate Caltrans overlay strategies for the rehabilitation of cracked asphalt concrete. It describes the results of the fourth HVS reflective cracking testing section, designated 588RF, carried out on a 90 mm full-thickness AR4000-D overlay, which was included as a control for performance comparison purposes. The test forms part of Partnered Pavement Research Center Strategic Plan Item 4.10: "Development of Improved Rehabilitation Designs for Reflective Cracking".

HVS trafficking on the section commenced on November 2, 2005 and was completed on April 11, 2006. A total of 1,410,000 load repetitions, equating to 37 million ESALs and a Traffic Index of 13.8, was applied during this period. A temperature chamber was used to maintain the pavement temperature at $20^{\circ}\text{C}\pm 4^{\circ}\text{C}$ for the first one million repetitions, then at $15^{\circ}\text{C}\pm 4^{\circ}\text{C}$ for the remainder of the test. A dual tire (720 kPa pressure) and bidirectional loading with lateral wander configuration was used. Findings and observations based on the data collected during this HVS study include:

- On completion of testing, the surface crack density was 9.1 m/m^2 and was mostly confined to one half of the section. Alligator cracking predominated on the overlay, similar to that on the underlying layer. The crack patterns of the two layers did not match exactly; however, the areas of most severe cracking corresponded.
- The average maximum rut depth across the entire test section at the end of the test was 15.9 mm. The rate of rutting was relatively slow during the early part of the experiment, but increased significantly after the 100 kN load change, despite reducing the pavement temperature to $15^{\circ}\text{C}\pm 4^{\circ}\text{C}$.
- Ratios of final-to-initial surface elastic deflections show that damage had increased significantly in the pavement structure by the end of trafficking, with loss of stiffness highest in the area of most severe cracking in the underlying layer.
- Analysis of surface profile measurements indicate that most of the permanent deformation probably occurred in the asphalt-bound surfacing layers (overlay and cracked DGAC) with the highest damage occurring in the area of most severe cracking in the underlying DGAC layer. No in-depth elastic deflection or permanent deformation data were collected due to problems with the MDDs. Malfunction was attributed to the loss of anchorage of the modules resulting from very wet conditions in the lower layers of the pavement and subgrade.
- Parts of the test were carried out during relatively high rainfall. This resulted in ponding of water adjacent to the section. Some pumping of fines through the cracks was noted in the final days of testing.

No recommendations as to the use of the modified binders in overlay mixes are made at this time. These recommendations will be included in the second-level analysis report, which will be prepared and submitted on completion of all HVS and laboratory testing.

Keywords:

Reflective cracking, overlay, modified binder, HVS test, MB Road

Related documents:

UCPRC-RR-2005-03, UCPRC-RR-2006-04, UCPRC-RR-2006-05, UCPRC-RR-2006-06

Signatures:

D. Jones 1st Author	J Harvey Technical Review	D. Spinner Editor	J. Harvey Principal Investigator	M Samadian Caltrans Contract Manager
------------------------	------------------------------	----------------------	-------------------------------------	---

DISCLAIMER

The contents of this report reflect the views of the authors who are responsible for the facts and accuracy of the data presented herein. The contents do not necessarily reflect the official views or policies of the State of California or the Federal Highway Administration. This report does not constitute a standard, specification, or regulation.

PROJECT OBJECTIVES

The objective of this project is to develop improved rehabilitation designs for reflective cracking for California.

This objective will be met after completion of four tasks identified by the Caltrans/Industry Rubber Asphalt Concrete Task Group (RACTG):

1. Develop improved mechanistic models of reflective cracking in California
2. Calibrate and verify these models using laboratory and HVS testing
3. Evaluate the most effective strategies for reflective cracking
4. Provide recommendations for reflective cracking strategies

This document is one of a series addressing Tasks 2 and 3.

ACKNOWLEDGEMENTS

The University of California Pavement Research Center acknowledges the assistance of the Rubber Pavements Association, Valero Energy Corporation, and Paramount Petroleum which contributed funds and asphalt binders for the construction of the Heavy Vehicle Simulator test track discussed in this study.

REFLECTIVE CRACKING STUDY REPORTS

The reports prepared during the reflective cracking study document data from construction, Heavy Vehicle Simulator (HVS) tests, laboratory tests, and subsequent analyses. These include a series of first- and second-level analysis reports and two summary reports. On completion of the study this suite of documents will include:

1. Reflective Cracking Study: Summary of Construction Activities, Phase 1 HVS testing and Overlay Construction (UCPRC-RR-2005-03).
2. Reflective Cracking Study: First-level Report on the HVS Rutting Experiment (UCPRC-RR-2007-06).
3. Reflective Cracking Study: First-level Report on HVS Testing on Section 590RF — 90 mm MB4-G Overlay (UCPRC-RR-2006-04).
4. Reflective Cracking Study: First-level Report on HVS Testing on Section 589RF — 45 mm MB4-G Overlay (UCPRC-RR-2006-05).
5. Reflective Cracking Study: First-level Report on HVS Testing on Section 587RF — 45 mm RAC-G Overlay (UCPRC-RR-2006-06).
6. Reflective Cracking Study: First-level Report on HVS Testing on Section 588RF — 90 mm AR4000-D Overlay (UCPRC-RR-2006-07).
7. Reflective Cracking Study: First-level Report on HVS Testing on Section 586RF — 45 mm MB15-G Overlay (UCPRC-RR-2006-12).
8. Reflective Cracking Study: First-level Report on HVS Testing on Section 591RF — 45 mm MAC15-G Overlay (UCPRC-RR-2007-04).
9. Reflective Cracking Study: HVS Test Section Forensic Report (UCPRC-RR-2007-05).
10. Reflective Cracking Study: First-level Report on Laboratory Fatigue Testing (UCPRC-RR-2006-08).
11. Reflective Cracking Study: First-level Report on Laboratory Shear Testing (UCPRC-RR-2006-11).
12. Reflective Cracking Study: Back Calculation of FWD Data from HVS Test Sections (UCPRC-RR-2007-08).
13. Reflective Cracking Study: Second-level Analysis Report (UCPRC-RR-2007-09).
14. Reflective Cracking Study: Summary Report (UCPRC-SR-2007-01). Detailed summary report.
15. Reflective Cracking Study: Summary Report (UCPRC-SR-2007-03). Four page summary report.

CONVERSION FACTORS

SI* (MODERN METRIC) CONVERSION FACTORS				
APPROXIMATE CONVERSIONS TO SI UNITS				
Symbol	Convert From	Multiply By	Convert To	Symbol
LENGTH				
in	inches	25.4	millimeters	mm
ft	feet	0.305	meters	m
AREA				
in ²	square inches	645.2	square millimeters	mm ²
ft ²	square feet	0.093	square meters	m ²
VOLUME				
ft ³	cubic feet	0.028	cubic meters	m ³
MASS				
lb	pounds	0.454	kilograms	kg
TEMPERATURE (exact degrees)				
°F	Fahrenheit	5 (F-32)/9 or (F-32)/1.8	Celsius	C
FORCE and PRESSURE or STRESS				
lbf	poundforce	4.45	newtons	N
lbf/in ²	poundforce/square inch	6.89	kilopascals	kPa
APPROXIMATE CONVERSIONS FROM SI UNITS				
Symbol	Convert From	Multiply By	Convert To	Symbol
LENGTH				
mm	millimeters	0.039	inches	in
m	meters	3.28	feet	ft
AREA				
mm ²	square millimeters	0.0016	square inches	in ²
m ²	square meters	10.764	square feet	ft ²
VOLUME				
m ³	cubic meters	35.314	cubic feet	ft ³
MASS				
kg	kilograms	2.202	pounds	lb
TEMPERATURE (exact degrees)				
C	Celsius	1.8C+32	Fahrenheit	F
FORCE and PRESSURE or STRESS				
N	newtons	0.225	poundforce	lbf
kPa	kilopascals	0.145	poundforce/square inch	lbf/in ²

*SI is the symbol for the International System of Units. Appropriate rounding should be made to comply with Section 4 of ASTM E380.
(Revised March 2003)

EXECUTIVE SUMMARY

This report is the fourth in a series of first-level analysis reports that describe the results of HVS testing on a full-scale experiment being performed at the Richmond Field Station (RFS) to validate Caltrans overlay strategies for the rehabilitation of cracked asphalt concrete. It describes the results of the fourth HVS reflective cracking testing section, designated 588RF, carried out on a 90-mm full-thickness dense-graded asphalt concrete (AR4000-D) overlay, which was included as one of the controls for performance comparison. The testing forms part of Partnered Pavement Research Center Strategic Plan Item 4.10: “Development of Improved Rehabilitation Designs for Reflective Cracking.”

The objective of this project is to develop improved rehabilitation designs for reflective cracking for California. This objective will be met after completion of the following four tasks:

1. Develop improved mechanistic models of reflective cracking in California
2. Calibrate and verify these models using laboratory and HVS testing
3. Evaluate the most effective strategies for reflective cracking
4. Provide recommendations for reflective cracking strategies

This report is one of a series addressing Tasks 2 and 3. It consists of three main chapters. Chapter 2 provides information on the experiment layout, pavement design, HVS trafficking of the underlying layer, and the test details, including test duration, pavement instrumentation and monitoring methods, loading program, test section failure criteria, and the environmental conditions recorded over the duration of the test. Chapter 3 summarizes the data collected and includes discussion of air and pavement temperatures during testing (measured with thermocouples), elastic deflection (measured on the surface with the Road Surface Deflectometer and at depth with Multi-depth Deflectometers), permanent deformation (measured on the surface with the Laser Profilometer and at depth with Multi-depth Deflectometers), and visual inspections. Chapter 4 provides a summary and lists key findings.

The underlying pavement was designed following standard Caltrans procedures and it incorporates a 410-mm (16.1 in) Class 2 aggregate base on subgrade with a 90-mm (3.5 in) dense-graded asphalt concrete (DGAC) surface. Design thickness was based on a subgrade R-value of 5 and a Traffic Index of 7 (~121,000 equivalent standard axles, or ESALs). This structure was trafficked with the HVS in 2003 to induce fatigue cracking then overlaid with six different treatments to assess their ability to limit reflective cracking. The treatments included:

- Half-thickness (45 mm) MB4 gap-graded overlay (referred to as “45 mm MB4-G” in this report)
- Full-thickness (90 mm) MB4 gap-graded overlay (referred to as “90 mm MB4-G” in this report)

- Half-thickness MB4 gap-graded overlay with minimum 15 percent recycled tire rubber (referred to as “MB15-G” in this report)
- Half-thickness MAC15TR gap-graded overlay with minimum 15 percent recycled tire rubber (referred to as “MAC15-G” in this report)
- Half-thickness rubberized asphalt concrete gap-graded overlay (RAC-G), included as a control for performance comparison purposes (the section discussed in this report)
- Full-thickness (90 mm) AR4000 dense-graded overlay (AR4000-D), included as a control for performance comparison purposes

The thickness for the AR4000-D overlay was determined according to Caltrans Test Method 356. The other overlay thicknesses were either the same or half of the AR4000-D overlay thickness. Details on construction and the first phase of trafficking are provided in an earlier report.

Laboratory fatigue and shear studies are being conducted in parallel with HVS testing. Results of these studies will be detailed in separate reports. Comparison of the laboratory and test section performance, including the results of a forensic investigation to be conducted when all testing is complete, will be discussed in a second-level report once the data from the studies have been collected and analyzed.

HVS trafficking on the section commenced on November 2, 2005, and was completed on April 11, 2006. During this period a total of 1,410,000 load repetitions at loads varying between 60 kN (13,500 lb) and 100 kN (22,500 lb) were applied, which equates to approximately 37 million ESALs, using the Caltrans conversion of $(\text{axle load}/18,000)^{4.2}$, and to a Traffic Index of 13.8. A temperature chamber was used to maintain the pavement temperature at $20^{\circ}\text{C}\pm 4^{\circ}\text{C}$ ($68^{\circ}\text{F}\pm 7^{\circ}\text{F}$) for the first one million repetitions, then at $15^{\circ}\text{C}\pm 4^{\circ}\text{C}$ ($59^{\circ}\text{F}\pm 7^{\circ}\text{F}$) for the remainder of the test. A dual tire (720 kPa [104 psi] pressure) and bidirectional loading with lateral wander was used.

Findings and observations based on the data collected during this HVS study include:

- Cracking was first observed after approximately 510,000 repetitions. On completion of testing, the surface crack density was 9.1 m/m^2 (2.77 ft/ft^2), with cracking occurring predominantly on one half of the section (Stations 8 to 15). The surface crack density reached 2.5 m/m^2 (0.76 ft/ft^2), the failure criterion set for the experiment, after about 900,000 load repetitions, but trafficking was continued to determine whether cracking would eventually spread to the remainder of the test section. Cracking on the overlay was predominantly transverse up until the 100 kN (22,500 lb) load change. Thereafter, an alligator cracking pattern was observed, similar to that on the underlying layer. The crack patterns of the two layers did not match exactly, however, the areas

of most severe cracking corresponded. Test pit investigations will provide insights into what influenced the cracking patterns observed. FWD testing revealed a weaker structure under the area of most severe cracking.

- The average maximum rut depth and average maximum deformation across the entire test section at the end of the test was 15.9 mm (0.63 in) and 8.8 mm (0.35 in) respectively. The average maximum rut was higher than the failure criterion of 12.5 mm (0.5 in) set for the experiment, reached after approximately 1.2 million repetitions. As indicated above, testing was continued to determine whether cracking would eventually spread to the remainder of the test section. The maximum rut depth measured on the section was 30 mm (1.18 in). The rate of rutting was relatively slow during the early part of the experiment, but increased significantly after the 100 kN (22,500 lb) load change, despite the pavement temperature being reduced to $15^{\circ}\text{C}\pm 4^{\circ}\text{C}$ ($59^{\circ}\text{F}\pm 7^{\circ}\text{F}$). The final surface rutting pattern of the overlay generally corresponds with the fatigue cracking pattern, and the deepest part of the rut occurred on that half of the section with the highest density of cracking in the underlying DGAC layer.
- The two failure criteria set for the experiment were reached within approximately 300,000 load repetitions of each other.
- Ratios of final-to-initial elastic surface deflections under a 60 kN (13,500 lb) wheel load increased by between four and eleven times along the length of the section, indicating significant damage in the pavement structure in terms of loss of stiffness. The ratio of final-to-initial deflections was inconsistent across the section, with significantly higher values in the area overlying the most severely cracked area.
- Analysis of surface profiles and experience from other sections where MDD data was available, indicate that most of the permanent deformation probably occurred in the asphalt-bound surfacing layers (overlay and cracked DGAC) with approximately twice as much damage occurring in the area of most severe cracking in the underlying DGAC layer. No in-depth elastic deflection or permanent deformation data were collected in this experiment due to problems with the MDDs. Malfunction was attributed to the loss of anchorage of the modules resulting from very wet conditions in the lower layers of the pavement and subgrade.
- Parts of the test were carried out during relatively high rainfall. This resulted in ponding of water adjacent to the section. Some pumping of fines through the cracks was noted in the final days of testing.

No recommendations as to the use of modified binders in overlay mixes are made at this time. These recommendations will be included in the second-level analysis report, which will be prepared and submitted on completion of all HVS and laboratory testing.

TABLE OF CONTENTS

EXECUTIVE SUMMARY	v
LIST OF TABLES	xi
LIST OF FIGURES	xii
1. INTRODUCTION	1
1.1. Objectives	1
1.2. Overall Project Organization	1
1.3. Structure and Content of This Report.....	4
1.4. Measurement Units.....	4
2. TEST DETAILS	5
2.1. Experiment Layout	5
2.2. Test Section Layout	5
2.2.1 Pavement Instrumentation and Monitoring Methods.....	8
2.3. Underlying Pavement Design	8
2.4. Summary of Testing on the Underlying Layer	9
2.5. Reflective Cracking Section Design.....	10
2.6. Test Summary.....	11
2.6.1 Test Section Failure Criteria.....	11
2.6.2 Environmental Conditions.....	11
2.6.3 Test Duration.....	12
2.6.4 Loading Program.....	12
2.6.5 Measurement Summary.....	13
3. DATA SUMMARY	17
3.1. Temperatures	17
3.1.1 Air Temperatures in the Temperature Control Unit.....	17
3.1.2 Outside Air Temperatures	18
3.1.3 Temperature in the Asphalt Concrete Layer	20
3.2. Rainfall	21
3.3. Elastic Deflection	21
3.3.1 Surface Elastic Deflection Using RSD.....	22
3.3.2 Surface Elastic Deflection Using FWD.....	27
3.3.3 In-Depth Elastic Deflection.....	30
3.4. Permanent Deformation.....	30
3.4.1 Permanent Surface Deformation (Rutting).....	31

3.4.2	Permanent In-Depth Deformation	37
3.5.	Visual Inspection	37
3.6.	Forensic Evaluation	44
3.7.	Second-Level Analysis	44
4.	CONCLUSIONS	45
5.	REFERENCES.....	49

LIST OF TABLES

Table 2.1: Summary of Load History.....	12
Table 2.2: Summary of MDD and RSD Measurements.....	15
Table 2.3: Summary of FWD Measurements.....	14
Table 3.1: Temperature Summary for Air and Pavement	20
Table 3.2: Average 60 kN RSD Centerline Deflections Before and After Testing.....	22
Table 3.3: Summary of FWD Measurements.....	27

LIST OF FIGURES

Figure 1.1: Timeline for the Reflective Cracking Study.	3
Figure 2.1: Layout of Reflective Cracking Study project.	6
Figure 2.2: Section 588RF layout and location of instruments.	7
Figure 2.2: Pavement design for the Reflective Cracking Study test track.	8
Figure 2.3: Cracking pattern on Section 569RF after Phase I HVS testing.	9
Figure 2.4: Gradation for AR4000-D overlay.	11
Figure 2.5: Cumulative traffic applications and loading history.	13
Figure 3.1: Frequencies of recorded temperatures.	18
Figure 3.2: Daily average air temperatures inside the temperature control chamber.	19
Figure 3.3: Daily average air temperatures outside the temperature control chamber.	19
Figure 3.4: Daily average temperatures at pavement surface and various depths.	20
Figure 3.5: Monthly rainfall for Richmond Field Station.	21
Figure 3.6: RSD deflections at CL locations with 60 kN test load at test start.	23
Figure 3.7: RSD deflections at CL locations with 60 kN test load after 215,000 repetitions.	23
Figure 3.8: RSD deflections at CL locations with 60 kN test load after 417,000 repetitions.	24
Figure 3.9: RSD deflections at CL locations with 60 kN test load after 1,005,600 repetitions.	24
Figure 3.10: RSD deflections at CL locations with 60 kN test load at test completion.	25
Figure 3.11: Average RSD surface deflections with 60 kN test load (centerline and sides).	26
Figure 3.12: Average RSD surface deflections with 60 kN test load (centerline and subsection).	26
Figure 3.13: Composite pavement stiffness (FWD Sensor 1) on section centerline.	28
Figure 3.14: Subgrade pavement stiffness (FWD Sensor 6) on section centerline.	29
Figure 3.15: Composite pavement stiffness (FWD Sensor 1) outside trafficked area.	29
Figure 3.16: Subgrade pavement stiffness (FWD Sensor 6) outside trafficked area.	30
Figure 3.17: Illustration of maximum rut depth and maximum deformation of a leveled profile.	31
Figure 3.18: Profilometer cross section at various load repetitions.	32
Figure 3.19: Average maximum deformation determined from Laser Profilometer data.	33
Figure 3.20: Average maximum rut determined from Laser Profilometer data.	33
Figure 3.21: Contour plot of permanent deformation after 215,000 repetitions.	34
Figure 3.22: Contour plot of permanent deformation after 417,000 repetitions.	34
Figure 3.23: Contour plot of permanent deformation after 861,000 repetitions.	35
Figure 3.24: Contour plot of permanent deformation after 1,006,000 repetitions.	35
Figure 3.25: Contour plot of permanent deformation after test completion.	36
Figure 3.26: Comparison of Phase 1 cracking pattern and Phase II rutting at test completion.	36

Figure 3.27: Photograph of Section 588RF showing cracks in one half of the section..... 39

Figure 3.28: Surface cracks marked with crayon between Stations 10 and 12 at end of test..... 40

Figure 3.29: Crack development between 510,000 and 910,000 repetitions. 41

Figure 3.30: Crack development between 990,000 repetitions and test completion. 42

Figure 3.31: Cracking pattern comparison between underlying layer and overlay..... 43

Figure 3.32: Crack accumulation with trafficking. 43

1. INTRODUCTION

1.1. Objectives

The first-level analysis presented in this report is part of Partnered Pavement Research Center Strategic Plan Element 4.10 (PPRC SPE 4.10) being undertaken for the California Department of Transportation (Caltrans) by the University of California Pavement Research Center (UCPRC). The objective of the study is to evaluate the reflective cracking performance of asphalt binder mixes used in overlays for rehabilitating cracked asphalt concrete pavements in California. The study includes mixes modified with rubber and polymers, and it will develop tests, analysis methods, and design procedures for mitigating reflective cracking in overlays. This work is part of a larger study on modified binder (MB) mixes being carried out under the guidance of the Caltrans Pavement Standards Team (PST) (1), which includes laboratory and accelerated pavement testing using the Heavy Vehicle Simulator (carried out by the UCPRC), and the construction and monitoring of field test sections (carried out by Caltrans).

1.2. Overall Project Organization

This UCPRC project is a comprehensive study, carried out in three phases, involving the following primary elements (2):

- Phase 1
 - The construction of a test pavement and subsequent overlays;
 - Six separate Heavy Vehicle Simulator (HVS) tests to crack the pavement structure;
 - Placing of six different overlays on the cracked pavement;
- Phase 2
 - Six HVS tests to assess the susceptibility of the overlays to high-temperature rutting (Phase 2a);
 - Six HVS tests to determine the low-temperature reflective cracking performance of the overlays (Phase 2b);
 - Laboratory shear and fatigue testing of the various hot-mix asphalts (Phase 2c);
 - Falling Weight Deflectometer (FWD) testing of the test pavement before and after construction and before and after each HVS test;
 - Forensic evaluation of each HVS test section;
- Phase 3
 - Performance modeling and simulation of the various mixes using models calibrated with data from the primary elements listed above.

Phase 1

In this phase, a conventional dense-graded asphalt concrete (DGAC) test pavement was constructed at the Richmond Field Station (RFS) in the summer of 2001. The pavement was divided into six cells, and within each cell a section of the pavement was trafficked with the HVS until the pavement failed by either fatigue (2.5 m/m^2 [0.76 ft/ft²]) or rutting (12.5 mm [0.5 in]). This period of testing began in the summer of 2001 and was concluded in the spring of 2003. In June 2003 each test cell was overlaid with either conventional DGAC or asphalt concrete with modified binders as follows:

- Full-thickness (90 mm) AR4000-D dense graded asphalt concrete overlay, included as a control for performance comparison purposes (AR-4000 is approximately equivalent to a PG64-16 performance grade binder);
- Full-thickness (90 mm) MB4-G gap-graded overlay;
- Half-thickness (45 mm) rubberized asphalt concrete gap-graded overlay (RAC-G), included as a control for performance comparison purposes;
- Half-thickness (45 mm) MB4-G gap-graded overlay;
- Half-thickness (45 mm) MB4-G gap-graded overlay with minimum 15 percent recycled tire rubber (MB15-G), and
- Half-thickness (45 mm) MAC15-G gap-graded overlay with minimum 15 percent recycled tire rubber.

The conventional overlay was designed using the current (2003) Caltrans overlay design process. The various modified overlays were either full (90 mm) or half thickness (45 mm). Mixes were designed by Caltrans. The overlays were constructed in one day.

Phase 2

Phase 2 included high-temperature rutting and low-temperature reflective cracking testing with the HVS as well as laboratory shear and fatigue testing. The rutting tests were started and completed in the fall of 2003. For these tests, the HVS was placed above a section of the underlying pavement that had not been trafficked during Phase 1. A reflective cracking test was next conducted on each overlay from the winter of 2003-2004 to the summer of 2007. For these tests, the HVS was positioned precisely on top of the sections of failed pavement from the Phase 1 HVS tests to investigate the extent and rate of crack propagation through the overlay.

In conjunction with Phase 2 HVS testing, a full suite of laboratory testing, including shear and fatigue testing, was carried out on field-mixed, field-compacted, field-mixed, laboratory-compacted, and laboratory-mixed, laboratory-compacted specimens.

Phase 3

Phase 3 entailed a second-level analysis carried out on completion of HVS and laboratory testing (the focus of this report). This included extensive analysis and characterization of the mix fatigue and mix shear data, backcalculation of the FWD data, performance modeling of each HVS test, and a detailed series of pavement simulations carried out using the combined data.

An overview of the project timeline is shown in Figure 1.1.

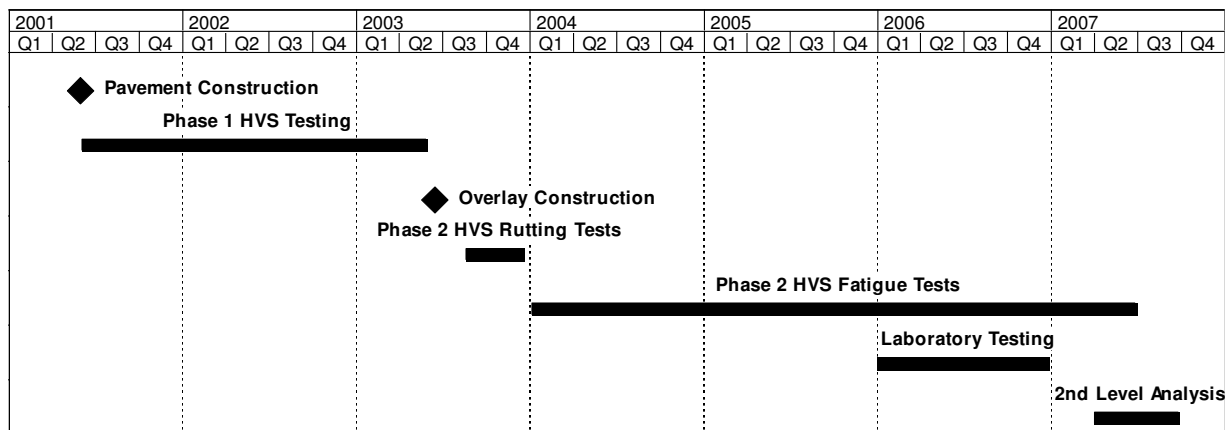


Figure 1.1: Timeline for the Reflective Cracking Study.

Reports

The reports prepared during the reflective cracking study document data from construction, HVS tests, laboratory tests, and subsequent analyses. These include a series of first- and second-level analysis reports and two summary reports. On completion of the study this suite of documents will include:

- One first-level report covering the initial pavement construction, the six initial HVS tests, and the overlay construction (Phase 1);
- One first-level report covering the six Phase 2 rutting tests (but offering no detailed explanations or conclusions on the performance of the pavements);
- Six first-level reports, each of which covers a single Phase 2 reflective cracking test (containing summaries and trends of the measured environmental conditions, pavement responses, and pavement performance but offering no detailed explanations or conclusions on the performance of the pavement);
- One first-level report covering laboratory shear testing;
- One first-level report covering laboratory fatigue testing;
- One report summarizing the HVS test section forensic investigation;
- One report summarizing the backcalculation analysis of deflection tests,

- One second-level analysis report detailing the characterization of shear and fatigue data, pavement modeling analysis, comparisons of the various overlays, and simulations using various scenarios (Phase 3), and
- One four-page summary report capturing the conclusions and one longer, more detailed summary report that covers the findings and conclusions from the research conducted by the UCPRC.

1.3. Structure and Content of This Report

This report presents the results of the HVS test on the full-thickness (90 mm) AR4000 dense-graded asphalt concrete overlay (referred to as “AR4000-D” in this report), designated Section 588RF, with preliminary analyses relative to observed performance and is organized as follows:

- Chapter 2 contains a description of the test program including experiment layout, loading sequence, instrumentation, and data collection.
- Chapter 3 presents a summary and discussion of the data collected during the test.
- Chapter 4 contains a summary of the results together with conclusions and observations.

1.4. Measurement Units

Metric units have always been used in the design and layout of HVS test tracks, and for all the measurements, data storage, analysis, and reporting at the eight HVS facilities worldwide (as well as all other international accelerated pavement testing facilities). Continued use of the metric system facilitates consistency in analysis, reporting, and data sharing.

In this report, metric and English units are provided in the Executive Summary, Chapters 1 and 2, and the Conclusion. In keeping with convention, only metric units are used in Chapter 3. A conversion table is provided on Page iv at the beginning of this report.

2. TEST DETAILS

2.1. Experiment Layout

Six overlays, each with a rutting test section and a reflective cracking test section, were constructed as part of the second phase of the study as follows:

1. Sections 580RF and 586RF: Half-thickness (45 mm) MB4 gap-graded overlay with minimum 15 percent recycled tire rubber (referred to as “MB15-G” in this report);
2. Sections 581RF and 587RF: Half-thickness (45 mm) rubberized asphalt concrete gap-graded (RAC-G) overlay;
3. Sections 582RF and 588RF: Full-thickness (90 mm) AR4000 dense-graded asphalt concrete overlay (designed using CTM356 and referred to as “AR4000-D” in this report);
4. Sections 583RF and 589RF: Half-thickness (45 mm) MB4 gap-graded overlay (referred to as “45 mm MB4-G” in this report);
5. Sections 584RF and 590RF: Full-thickness (90 mm) MB4 gap-graded overlay (referred to as “90 mm MB4-G” in this report), and
6. Sections 585RF and 591RF: Half-thickness (45 mm) MAC15TR gap-graded overlay with minimum 15 percent recycled tire rubber (referred to as “MAC15-G” in this report).

These sections and the corresponding Phase 1 fatigue test sections are shown in Figure 2.1. Prior to the Phase 2 reflective cracking testing, a rutting study was carried out whereby HVS loading at high temperature was applied adjacent to the reflective cracking experiments to evaluate the rutting behavior of the overlay mixes. The rutting study will be discussed in a separate report.

2.2. Test Section Layout

The test section layout for Section 591RF is shown in Figure 2.2. Station numbers refer to fixed points on the test section and are used for measurements and as a reference for discussing performance.

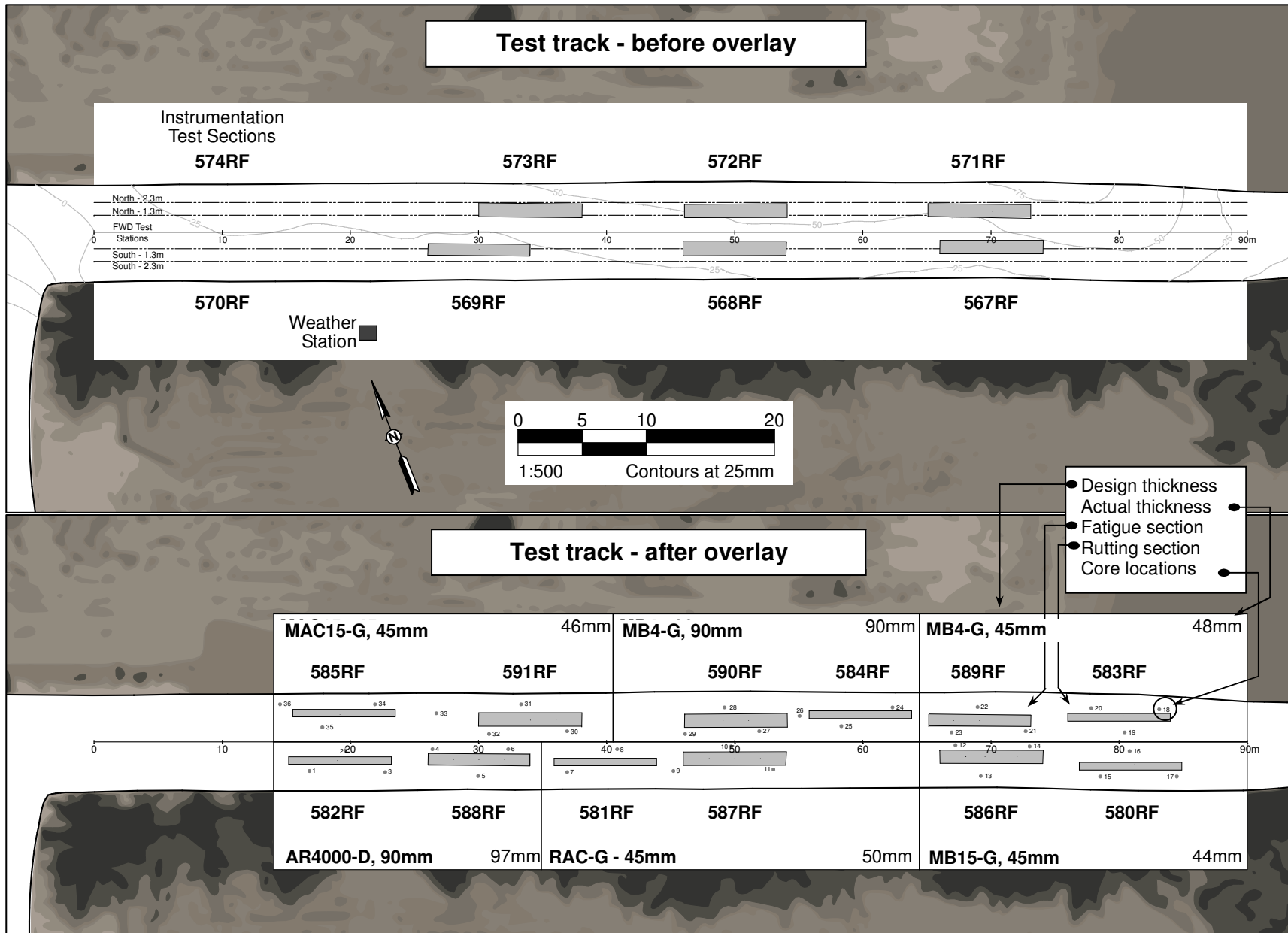


Figure 2.1: Layout of Reflective Cracking Study project.

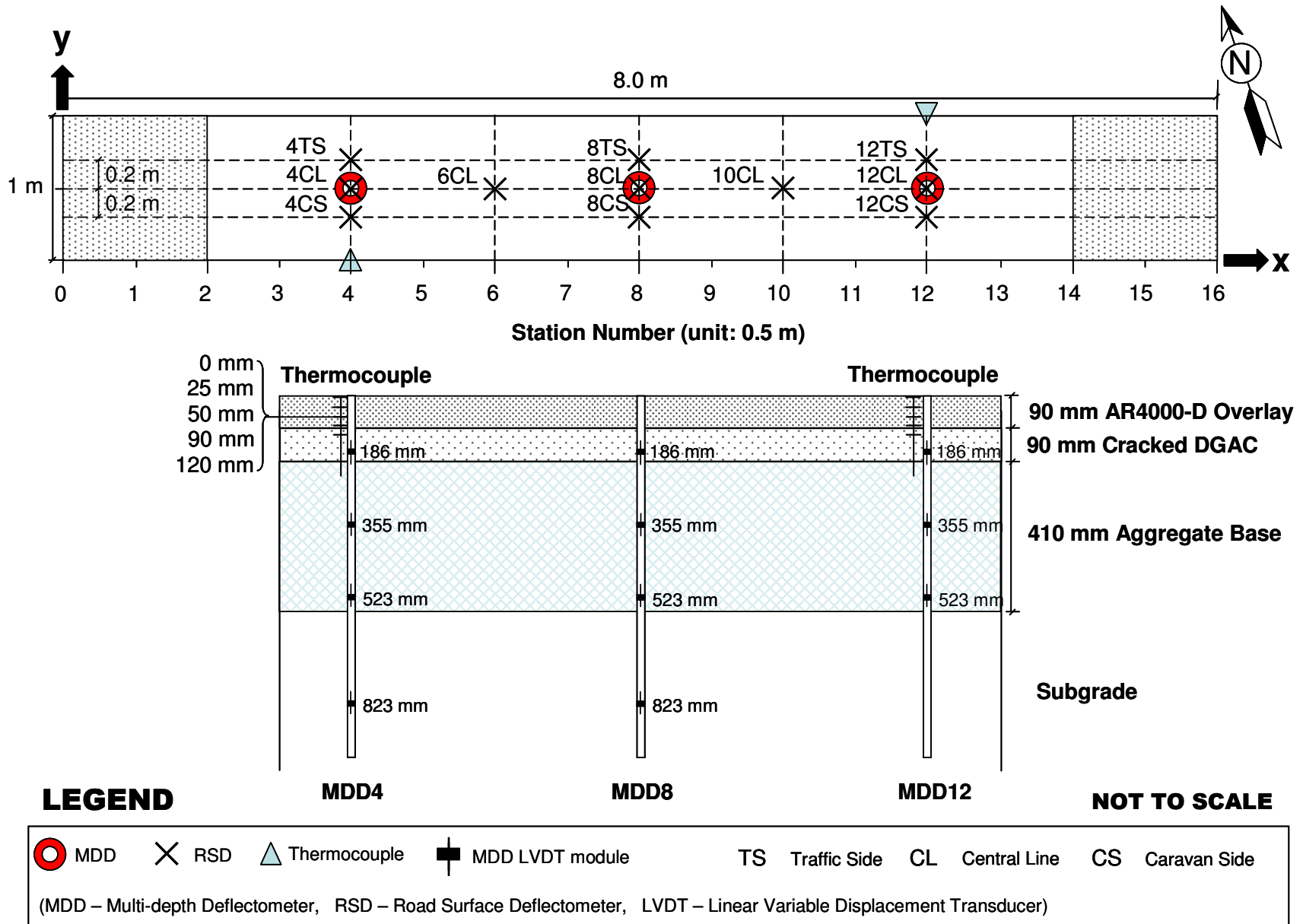


Figure 2.2: Section 588RF layout and location of instruments.

2.2.1 Pavement Instrumentation and Monitoring Methods

Measurements were taken with the following instruments:

- Road Surface Deflectometer (RSD), measuring surface deflection;
- Multi-depth Deflectometer (MDD), measuring elastic deflection and permanent deformation at different depths in the pavement;
- Laser Profilometer, measuring surface profile (at each station);
- Falling Weight Deflectometer (FWD), measuring elastic deflection before and after testing, and
- Thermocouples, measuring pavement temperature and ambient temperature.

Instrument positions are shown in Figure 2.2. Detailed descriptions of the instrumentation and measuring equipment are included in Reference 4. Intervals between measurements, in terms of load repetitions, were selected to enable adequate characterization of the pavement as damage developed.

2.3. Underlying Pavement Design

The pavement for the first phase of HVS trafficking was designed according to the Caltrans Highway Design Manual Chapter 600 using the computer program *NEWCON90*. Design thickness was based on a tested subgrade R-value of 5 and a Traffic Index of 7 (~121,000 ESALs) (3). The pavement design for the test road and the preliminary as-built pavement structure for Section 588RF (determined from cores removed from the edge of the section) are illustrated in Figure 2.3.

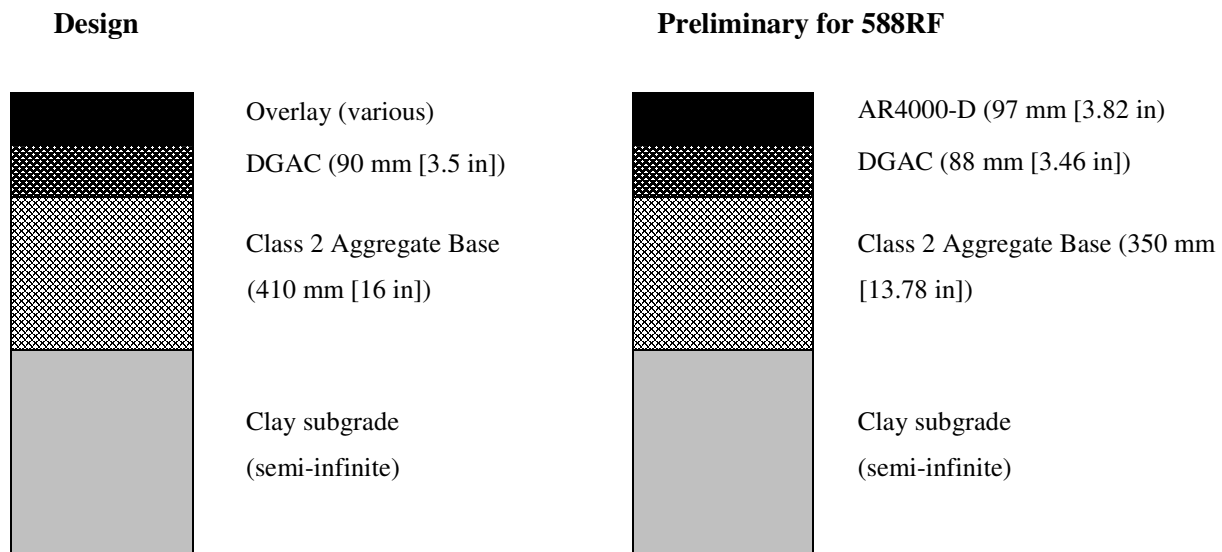


Figure 2.2: Pavement design for the Reflective Cracking Study test track.
(Design and preliminary actual for 588RF)

The existing subgrade was ripped and reworked to a depth of 200 mm (8 in) so that the optimum moisture content and the maximum wet density met the specification per Caltrans Test Method CTM 216. The average maximum wet density of the subgrade was 2,180 kg/m³ (136 pcf). The average relative compaction of the subgrade was 97 percent (3).

The aggregate base was constructed to meet the Caltrans compaction requirements for aggregate base Class 2 using CTM 231 nuclear density testing. The maximum wet density of the base determined according to CTM 216 was 2,200 kg/m³ (137 pcf). The average relative compaction was 98 percent.

The DGAC layer consisted of a dense-graded asphalt concrete (DGAC) with AR-4000 binder and aggregate gradation limits following Caltrans 19-mm (0.75 in) maximum size coarse gradation (3). The target asphalt content was 5.0 percent by mass of aggregate, while actual contents varied between 4.34 and 5.69 percent. Nuclear density measurements and extracted cores were used to determine a preliminary as-built mean air-void content of 9.1 percent with a standard deviation of 1.8 percent. The air-void content after traffic compaction and additional air-void contents from cores taken outside the trafficked area will be determined on completion of trafficking of all sections and will be reported in the second-level analysis report.

2.4. Summary of Testing on the Underlying Layer

Trafficking of the underlying Section 569RF took place between March 25, 2003, and April 11, 2003, during which 217,116 repetitions were applied. Figure 2.3 presents the final cracking pattern after testing. An alligator cracking pattern dominated. Total crack length was 36.33 m (119.19 ft) and crack density was 6.05 m/m² (1.84 ft/ft²).

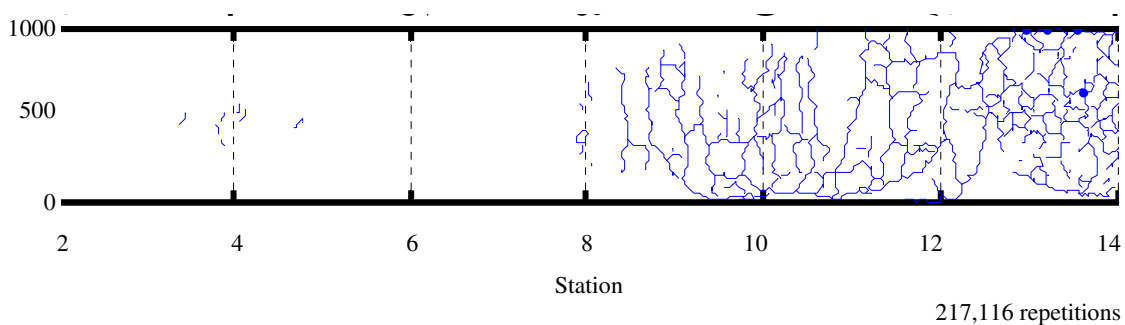


Figure 2.3: Cracking pattern on Section 569RF after Phase I HVS testing.

2.5. Reflective Cracking Section Design

Section 588RF was located on the 90-mm dense-graded asphalt concrete (DGAC) overlay precisely on top of Section 569RF. Section 569RF had significant alligator cracking over approximately half of the area subjected to HVS trafficking (Figure 2.3). The overlay thickness for the experiment was determined according to Caltrans Test Method CTM 356 using Falling Weight Deflectometer data from the Phase 1 experiment. The actual layer thickness of Section 588RF was measured from cores extracted from the edge of the test section and from Dynamic Cone Penetrometer (DCP) tests. The measured average thicknesses for the section from cores and DCP measurements taken outside the trafficked area were:

- AR4000-D Overlay: 97 mm (min 85 mm; max 105 mm; standard deviation, 8.6 mm)
[3.8 in (min 3.3 in; max 4.1 in; standard deviation, 0.3 in)]
- Cracked AR4000-D layer: 88 mm (min 85 mm; max 103 mm; standard deviation, 8.0 mm)
[3.5 in (min 3.3 in; max 4.1 in; standard deviation, 0.3 in)]
- Aggregate base: 350 mm (13.8 in)

Exact layer thicknesses will be determined from measurements in test pits after HVS testing has been completed on all sections.

Laboratory testing was carried out by Caltrans and UCPRC on samples collected during construction to determine actual binder properties, binder content, aggregate gradation, and air-void content. The AR4000-D binder met the Caltrans binder specification, based on testing performed by Caltrans. The ignition-extracted binder content, corrected for aggregate ignition, showed an average value of 6.13 percent, considerable higher than the design binder content of 5.0 percent. The aggregate gradation generally met Caltrans specifications for a 19.0 mm (3/4 inch) maximum size course gradation, with material passing the 0.6 mm (#30), 2.36 mm (#8) and 4.75 mm (#4) sieves on the envelope limits. Gradation is illustrated in Figure 2.4. The preliminary as-built air-void content was 7.1 percent with a standard deviation of 1.5 percent, based on cores taken outside of the HVS sections. Final air-void contents will be determined from trenching and coring to be performed after trafficking of all sections.

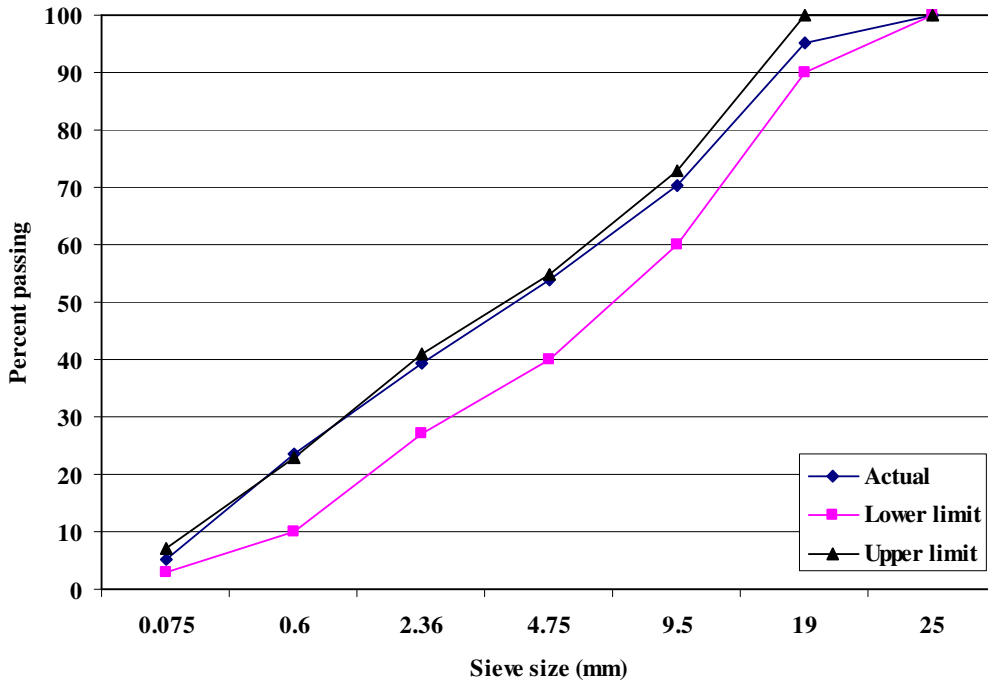


Figure 2.4: Gradation for AR4000-D overlay.

2.6. Test Summary

2.6.1 Test Section Failure Criteria

Failure criteria for analyses were set at:

- Cracking density of 2.5 m/m^2 (0.76 ft/ft^2) or more, and/or
- Average maximum surface rut depth of 12.5 mm (0.5 in) or more.

2.6.2 Environmental Conditions

For the first one million repetitions, the pavement surface temperature was maintained at $20^\circ\text{C} \pm 4^\circ\text{C}$ ($68^\circ\text{F} \pm 7^\circ\text{F}$) to minimize rutting in the asphalt concrete and to promote fatigue damage. Thereafter, the pavement surface temperature was reduced to $15^\circ\text{C} \pm 4^\circ\text{C}$ ($59^\circ\text{F} \pm 7^\circ\text{F}$) to further accelerate fatigue damage. A temperature control chamber (5) was used to maintain the test temperatures.

The pavement surface received no direct rainfall as it was protected by the temperature control chamber. The section was tested predominantly during the wet season (November to April) and hence water infiltration into the pavement from the side drains and through the raised groundwater table was possible.

2.6.3 Test Duration

HVS trafficking on Section 588RF was initiated on November 2, 2005, and completed on April 11, 2006, after the application of 1,410,000 load repetitions. Testing was interrupted three times:

- During a breakdown between November 7 and November 15, 2005, when the cumulative traffic repetitions were approximately 15,000;
- During the holiday shutdown and a subsequent breakdown between December 16, 2005 and January 8, 2006, when the repetition count was approximately 315,000, and
- During a breakdown between March 2 and March 6, 2006, when the repetition count was approximately 861,000.

2.6.4 Loading Program

The HVS test program is summarized in Table 2.1.

Table 2.1: Summary of Load History

Start Date	Start Repetition	Wheel Load (kN) - [lb]		Wheel	Tire Pressure (kPa) - [psi]	Direction
		Planned	Actual			
11/02/05 ¹	0	40 - [9,000]	60	Dual	720 - [104]	Bi
12/10/05	215,000	60 - [13,500]	90	Dual	720 - [104]	Bi
01/23/06 ²	417,000	80 - [18,000]	80	Dual	720 - [104]	Bi
03/14/06 ³	1,005,600	100 - [22,500]	100	Dual	720 - [104]	Bi

¹ Testing was interrupted during a breakdown between 11/07/05 and 11/15/05.
² Testing was interrupted during holiday shutdown and breakdown between 12/16/05 and 01/08/06.
³ Testing was interrupted during a breakdown between 03/02/06 and 03/06/06.

The loading program followed differs from the original test plan due to an incorrect hydraulic control system setup on loads less than 65 kN (14,600 lb) in the Phase 1 experiment. The loading pattern from the Phase 1 experiment was thus retained to facilitate comparisons of performance between all tests in the Reflective Cracking Study. Testing was undertaken with a dual-wheel configuration, using radial truck tires (Goodyear G159 - 11R22.5 - steel belt radial) inflated to a pressure of 720 kPa (104 psi), in a bidirectional loading mode. Lateral wander over the one-meter (39.4 in) width of the test section was programmed to simulate traffic wander on a typical highway lane.

Cumulative traffic applications and the loading history are shown in Figure 2.5. The shorter 60 kN (13,500 lb) and 90 kN (20,250 lb) and longer 80 kN (18,000 lb) and 100 kN (22,500 lb) loading phases adopted for Section 589 (second HVS test) were also used in this test. A total of 1,410,000 load repetitions were applied consisting of:

- 215,000 repetitions of a 60 kN (13,500 lb) load;
- 202,000 repetitions of a 90 kN (20,250 lb) load;
- 588,600 repetitions of an 80 kN (18,000 lb) load, and

- 404,400 repetitions of a 100 kN (22,500 lb) load.

This loading equates to approximately 37 million equivalent standard axles, using the Caltrans conversion of $(\text{axle load}/18000)^{4.2}$, which in turn equates to a Traffic Index of 13.8.

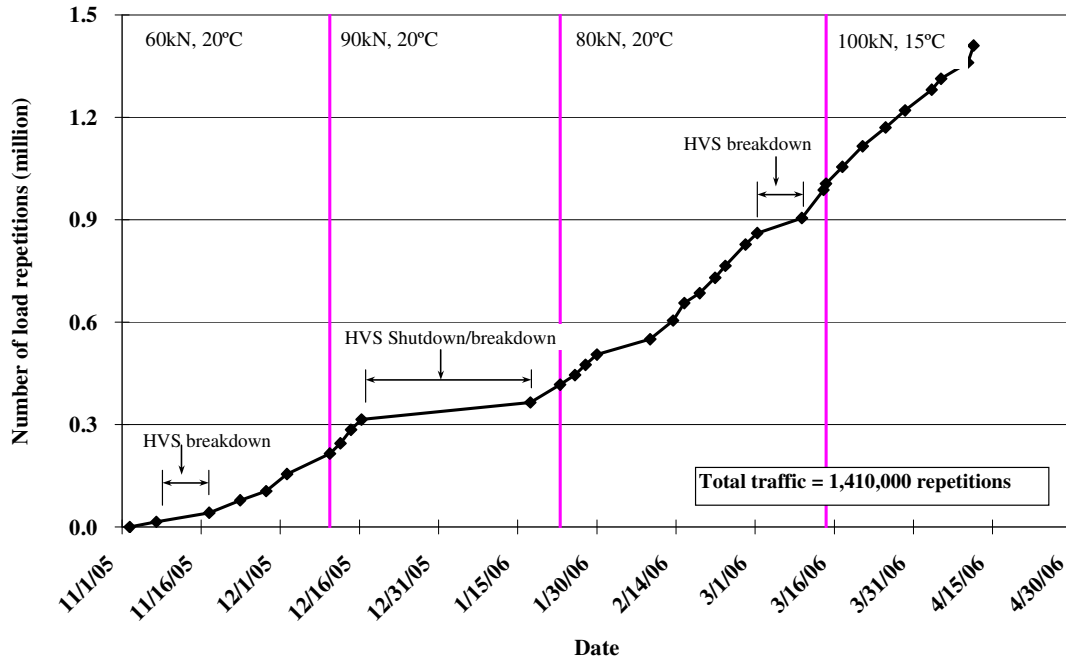


Figure 2.5: Cumulative traffic applications and loading history.

2.6.5 Measurement Summary

Table 2.2 (pages 15 and 16) lists the reading schedule of MDD and RSD measurements at various wheel loads. Surface deflection measurements with the RSD were obtained at the reference points along the centerline (CL) of the section and at locations 200 mm (8.0 in) on either side of the centerline (traffic and caravan side), as shown in Figure 2.2. MDD and RSD measurements were taken with a 60 kN (13,500 lb) load throughout the test as well as with the load being applied at the time of measurement (i.e., 80 kN [18,000 lb], 90 kN [22,500 lb], or 100 kN [22,500 lb]). The figures in Chapter 3 only show the measurements taken with the 60 kN (13,500 lb) load.

Measurements of surface rut depth taken by transverse scans with the Laser Profilometer were obtained at each station (Figure 2.2) on the same schedule as that of the MDD and RSD. The following rut parameters, which are discussed in more detail in Chapter 3, were determined from these measurements:

- Location and magnitude of the maximum rut depth,
- Average rut depth for the entire test section, and
- Rate of rut development.

Falling Weight Deflectometer (FWD) measurements were taken before and after testing at the center of and on the outside of the trafficked area. A summary of the measurement schedule is provided in Table 2.3.

Table 2.3: Summary of FWD Measurements

Date	Time	Location	Interval (m) - [ft]
10/19/05	06:55	Center & side	0.3 - [1.0]
10/19/05	14:38	Center & side	0.3 - [1.0]
04/28/06	12:50	Center & side	0.9 - [3.0]
04/28/06	14:47	Center & side	0.9 - [3.0]

Pavement temperature measurements were derived from thermocouples (depths and surface locations shown in Figure 2.2) at one-hour intervals during HVS operation. Air temperatures were measured in a weather station next to the test section and recorded at the same intervals as the thermocouples.

Crack development was monitored using visual inspection of the road surface and photographs.

Table 2.2: Summary of MDD and RSD Measurements

Date	Reps (x1m)	Temp (°C)	MDD4				MDD8				MDD12				RSD Center line ¹				RSD Sides ²							
			60*	90	80	100	60	90	80	100	60	90	80	100	60	90	80	100	60	90	80	100				
11/02/05	0.000	17.5	x				x				x				✓				✓							
11/07/05	0.015	17.5	x				x				x				✓											
11/17/05	0.042	18.6	x				x				x				✓											
11/23/05	0.078	16.5	x				x				x				✓											
11/28/05	0.110	14.0	x				x				x				✓											
12/02/05	0.155	13.3	x				x				x				✓											
12/10/05	0.215	16.4	x	x			x	x			x	x			✓	✓			✓	✓						
12/12/05	0.245	16.3	x	x			x	x			x	x			✓	✓										
12/14/05	0.285	15.6	x	x			x	x			x	x			✓	✓										
12/16/05	0.315	13.8	x	x			x	x			x	x			✓	✓										
01/17/06	0.365	13.3	x	x			x	x			x	x			✓	✓										
01/23/06	0.417	13.8	x	x	x		x	x	x		x	x	x		✓	✓	✓		✓	✓	✓					
01/25/06	0.445	14.4	x		x		x				x		x		✓		✓									
01/27/06	0.475	13.5	x		x		x				x		x		✓		✓									
01/30/06	0.505	13.8	x		x		x				x		x		✓		✓									
02/09/06	0.550	16.6	x		x		x				x		x		✓		✓									
02/13/06	0.605	16.4	x		x	x	x				x	x	x		✓		✓	✓	✓	✓	✓	✓				
02/15/06	0.656	13.9	x		x	x	x				x	x	x		✓		✓	✓								
02/18/06	0.685	12.8	x		x	x	x				x	x	x		✓		✓	✓								
02/21/06	0.730	11.6	x		x	x	x				x	x	x		✓		✓	✓								
02/23/06	0.765	14.7	x		x	x	x				x	x	x		✓		✓	✓								
02/27/06	0.827	13.5	x		x	x	x				x	x	x		✓		✓	✓								
03/01/06	0.861	13.8	x		x	x	x				x	x	x		✓		✓	✓								
03/09/06	0.905	13.8	x		x	x	x				x	x	x		✓		✓	✓								
03/13/06	0.987	11.5	x		x	x	x				x	x	x		✓		✓	✓								
03/14/06	1.005	11.9	x	x	x	x	x	x	x	x	x	x	x	✓	x	✓	✓	✓	✓	✓	✓	✓				
03/17/06	1.055	14.1	x		x	x	x				x	x	x		✓		✓	✓								
03/21/06	1.115	13.8	x		x	x	x				x	x	x		✓		✓	✓								
03/25/06	1.117	13.4	x		x	x	x				x	x	x		✓		✓	✓								
03/29/06	1.220	13.7	x		x	x	x				x	x	x		✓		✓	✓								
04/03/06	1.281	13.1	x		x	x	x				x	x	x		✓		✓	✓								
04/05/06	1.313	12.8	x		x	x	x				x	x	x		✓		✓	✓								
04/10/06	1.360	16.9	x		x	x	x				x	x	x		✓		✓	✓								
04/11/06	1.410	16.9	x		x	x	x				x	x	x		✓		✓	✓	✓	✓	✓	✓				
* Wheel load in kN			¹ Measurements at 4, 6, 8, 10, and 12								² Measurements at 4, 8, and 12															
✓	Data collected		x								Suspect data, not used								No data collection scheduled							

3. DATA SUMMARY

This chapter provides a summary of the data collected from Section 588RF and a brief discussion of the first-level analysis. Interpretation of the data in terms of pavement performance will be discussed in a separate second-level analysis report.

3.1. Temperatures

Pavement temperatures were controlled using the temperature control chamber. Both air (inside and outside the temperature box) and pavement temperatures were monitored and recorded hourly during the entire loading period. Figure 3.1 illustrates the frequencies of recorded temperatures at each hour in the testing period from November 2, 2005 to April 11, 2006, a total of 160 days. Hourly temperatures were collected for approximately 75 percent of the test period. No temperatures were recorded during the periods of breakdown. As seen in the figure, the hour counts from 08:00 to 14:00 hours (on a 24-hour clock) are relatively low, this being the period when measurements were taken. As a consequence, temperature interpolation/extrapolation will be necessary when interpreting the backcalculation results from the Multi-Depth Deflectometer (MDD) and Road Surface Deflectometer (RSD) measurements (second-level analysis). In assessing fatigue performance, the temperature at the bottom of the asphalt concrete and the temperature gradient are the two important controlling temperature parameters used to evaluate the stiffness of the asphalt concrete and to compute the maximum tensile strain as accurately as possible.

3.1.1 Air Temperatures in the Temperature Control Unit

Air temperatures inside the temperature control chamber ranged from 8°C to 23°C during the entire testing period. Temperatures were adjusted to maintain a pavement temperature at 50 mm depth of 20°C±4°C for the first one million repetitions and 15°C±4°C for the remainder of the test. These temperature ranges are expected to promote fatigue damage leading to reflective cracking while minimizing rutting of the asphalt concrete layer. The temperature distributions for the various stages of the test were:

- Zero to one million repetitions: mean of 15.0°C with a standard deviation of 2.9°C, and
- One million to end of test: mean of 14.0°C with a standard deviation of 1.3°C.

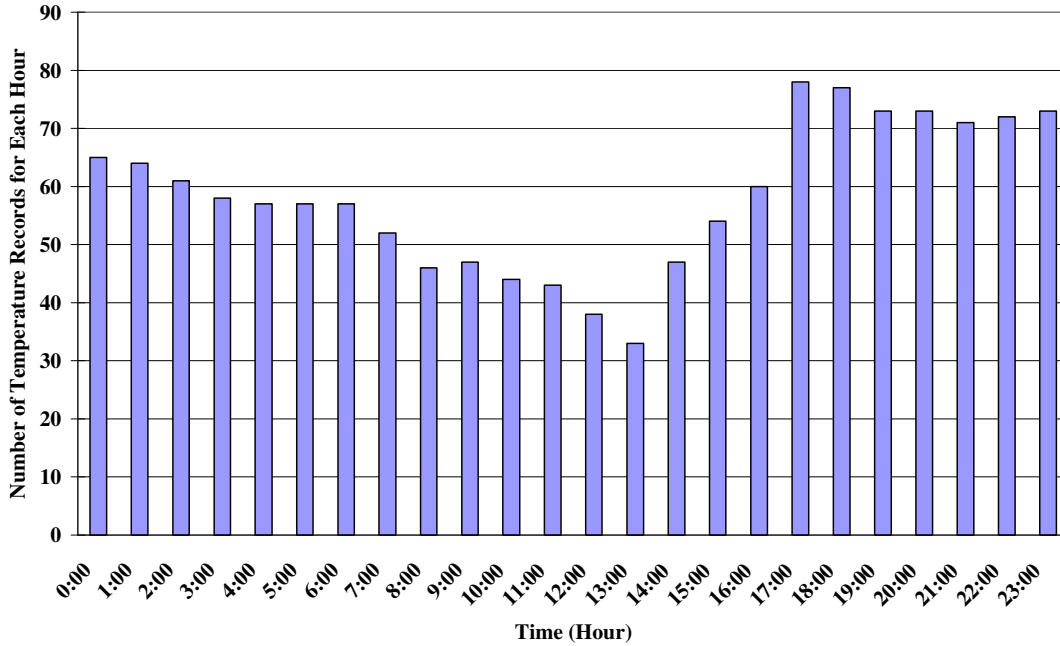


Figure 3.1: Frequencies of recorded temperatures.

The daily average temperatures recorded in the temperature control unit, calculated from the hourly temperatures recorded during HVS operation, are shown in Figure 3.2. Vertical errors bars on each point on the graph show daily temperature range.

3.1.2 Outside Air Temperatures

Outside air temperatures ranged from 1.0°C to 27.0°C with an average of 11.0 C (standard deviation of 2.8°C) during the test period and are summarized in Figure 3.3. Vertical error bars on each point on the graph show daily temperature range. The temperature distributions for the various stages of the test were:

- Entire duration: mean of 11.0°C with a standard deviation 2.8°C, and lowest and highest temperatures of 1.0°C and 27°C respectively;
- Zero to one million repetitions: mean of 11.0°C with a standard deviation of 3.2°C, and lowest and highest temperatures of 1.0°C and 27.0°C respectively, and
- One million to end of test: mean of 11.0°C with a standard deviation of 1.2°C, and lowest and highest temperatures of 4.0°C and 23.0°C respectively.

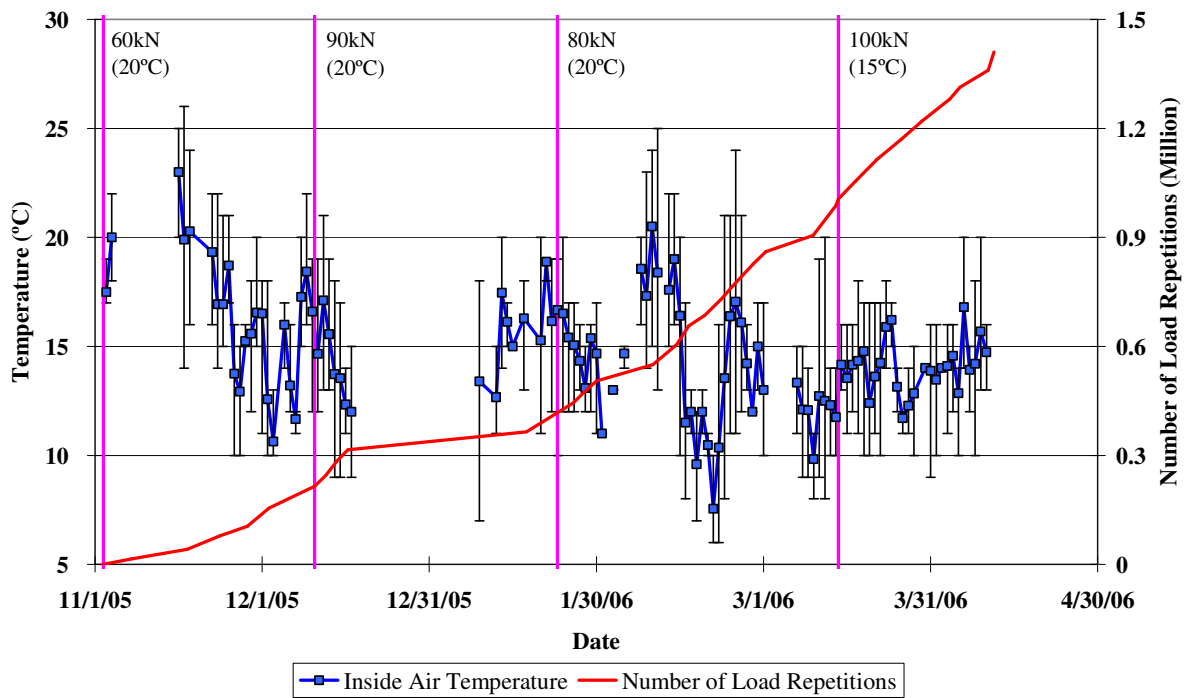


Figure 3.2: Daily average air temperatures inside the temperature control chamber.

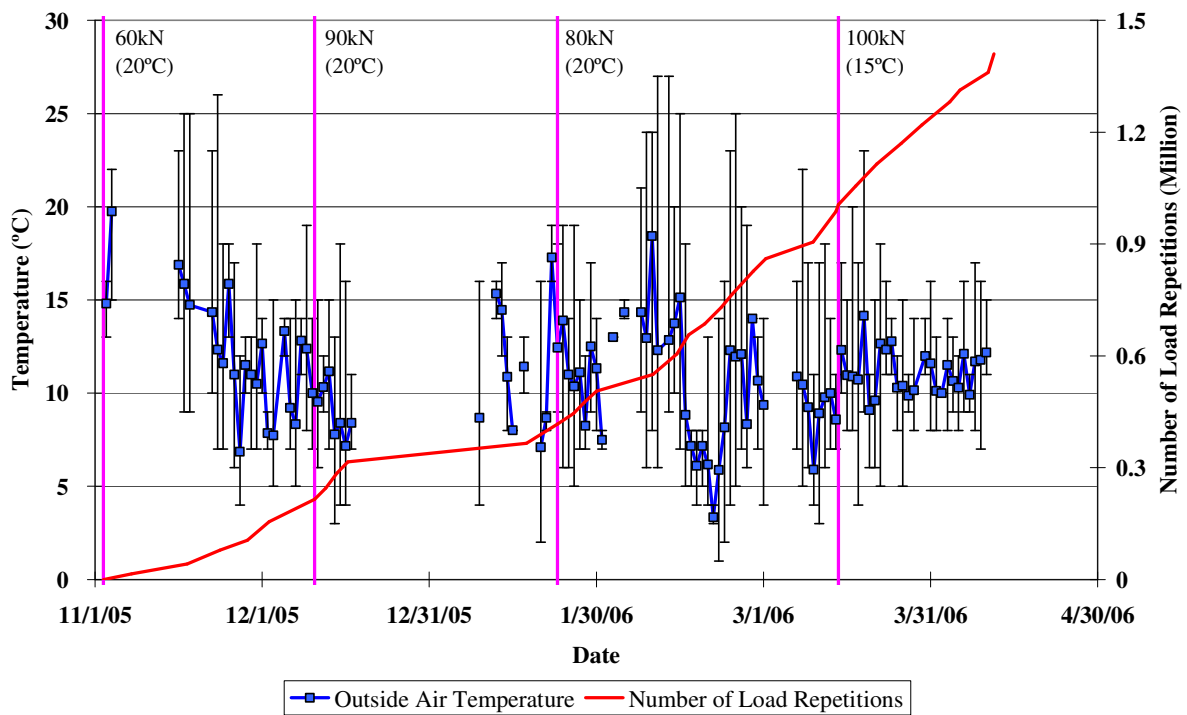


Figure 3.3: Daily average air temperatures outside the temperature control chamber.

3.1.3 Temperature in the Asphalt Concrete Layer

Daily averages of the surface and in-depth temperatures are listed in Table 3.1 and shown in Figure 3.4. Pavement temperatures decreased slightly during the course of the experiment with very little difference (<0.5°C) in temperature at the various depths. After one million repetitions, pavement temperatures dropped by 0.5°C in the upper 50 mm of the pavement, by 0.4°C between 50 and 100 mm depth, and by 0.3°C below 100 mm. There was again little difference at the various depths. Pavement temperatures did not appear to be significantly influenced by outside air temperatures.

Table 3.1: Temperature Summary for Air and Pavement

Temperature location	Overall		0 - 1,000,000		1,000,000 - 1,410,000	
	Average (°C)	Std Dev (°C)	Average (°C)	Std Dev (°C)	Average (°C)	Std Dev (°C)
Outside air	11.0	2.8	11.0	3.2	11.0	1.2
Inside air	14.7	2.6	15.0	2.9	14.0	1.3
Pavement surface	14.5	1.8	14.6	2.0	14.1	1.3
- 25-mm below surface	14.5	1.8	14.6	1.9	14.1	1.3
- 50-mm below surface	14.3	1.7	14.5	1.5	14.0	1.2
- 90-mm below surface	14.2	1.6	14.3	1.7	13.9	1.2
- 120-mm below surface	14.1	1.6	14.1	1.7	13.8	1.2

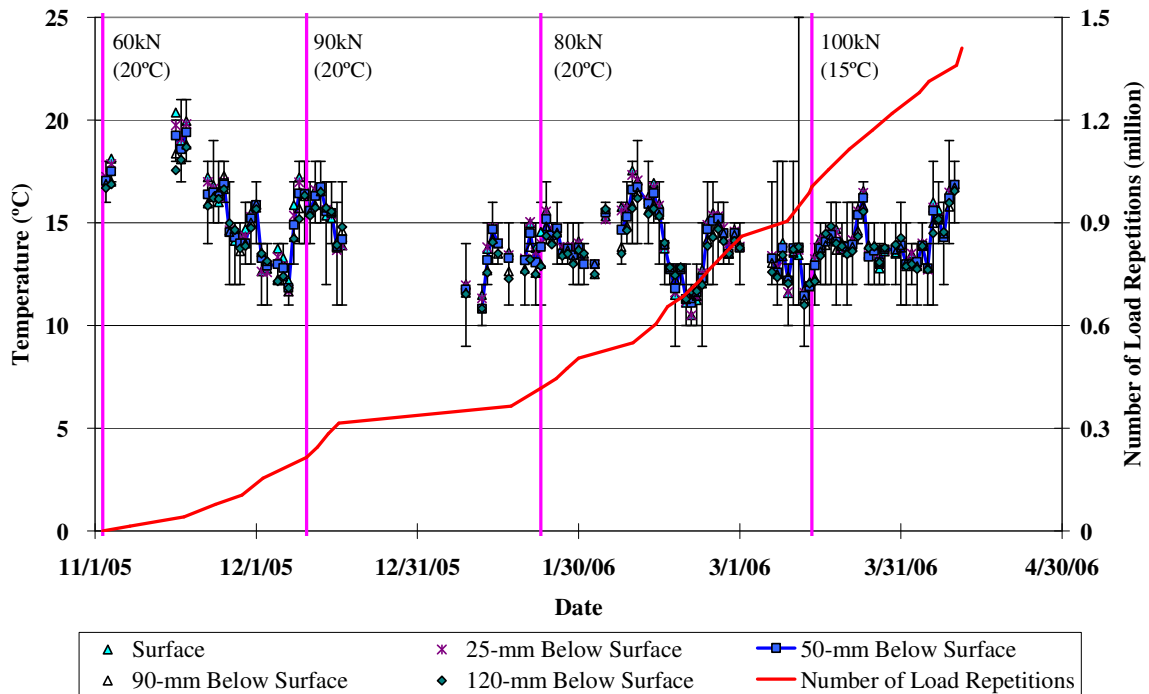


Figure 3.4: Daily average temperatures at pavement surface and various depths.

3.2. Rainfall

Figure 3.5 shows the monthly rainfall data from October 2005 to April 2006 as adapted from the Richmond Field Station HVS site recording station. Relatively high rainfall was recorded during the months of December 2005 and March 2006 and standing water was often observed on the sides of the test road.

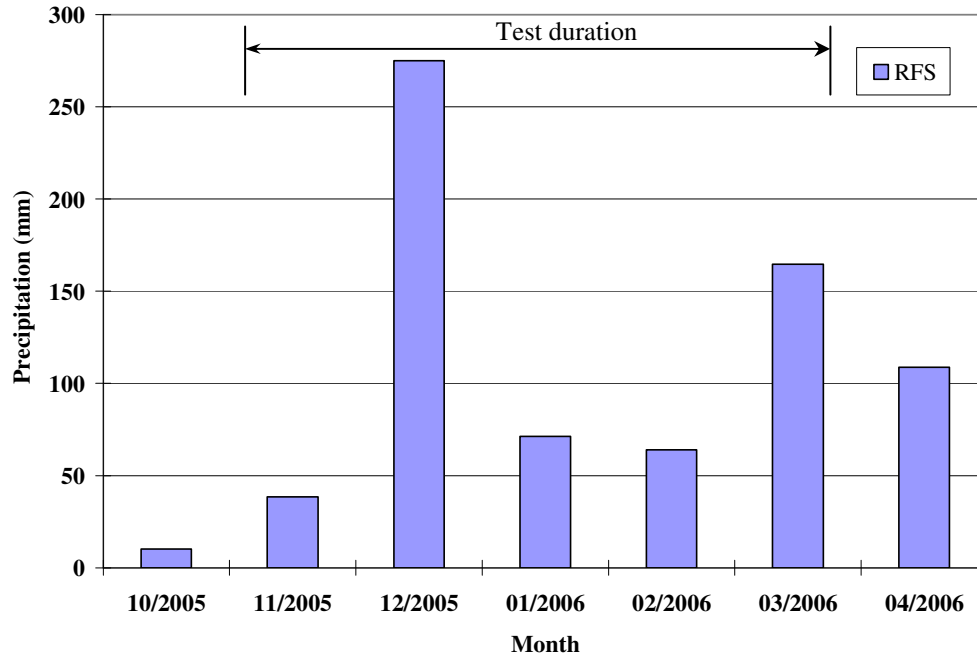


Figure 3.5: Monthly rainfall for Richmond Field Station.

3.3. Elastic Deflection

Elastic (recoverable) deflections provide an indication of the overall stiffness of the pavement structure and, therefore, a measure of the load-carrying capacity. As the stiffness of a pavement structure deteriorates, its ability to resist the deformation/deflection caused by a given load and tire pressure decreases. During HVS testing elastic deflections are measured with two instruments: the RSD to measure surface deflections and the MDD to measure in-depth deflections. MDD modules could not be installed at the surface (0 mm) due to the limited thickness of the overlay and thus it is not possible to directly compare surface deflections between the two instruments. In addition to RSD and MDD measurements, Falling Weight Deflectometer (FWD) measurements were taken before and after HVS trafficking to evaluate the initial and final conditions of the pavement.

3.3.1 Surface Elastic Deflection Using RSD

In this section of the report, surface deflections as measured by the RSD under a load of 60 kN are summarized (note that the HVS trafficking load does not remain the same during the course of the experiment).

Table 3.2 compares the average 60 kN RSD deflections for centerline locations 4CL, 6CL, 8CL, 10CL, and 12CL before and on completion of testing. The high standard deviation for the average deflection after trafficking is attributed to variability in the cracking of the underlying Dense Graded Asphalt Concrete (DGAC) layer, which is discussed below.

Table 3.2: Average 60 kN RSD Centerline Deflections Before and After Testing

Position	Parameter	Deflection (microns)		
		Before Trafficking	After Trafficking	Ratio of Final/Initial
All	Average	257	2,099	8.17
	Std. Deviation	38	941	-
4CL	Average	217	969	4.47
6CL	Average	240	1,205	5.02
8CL	Average	234	2,720	11.62
10CL	Average	286	3,027	10.58
12CL	Average	309	2,573	8.33

At the start of the test, initial deflections were all within 0.09 mm of each other, with higher deflections (i.e., weaker pavement) recorded at positions 10CL and 12CL compared to 4CL, 6CL, and 8CL. During the course of the test, substantial damage occurred on the overlay over the entire section under HVS trafficking, with higher values recorded between 8CL and 12CL. This is confirmed by the ratio of final-to-initial deflections for all RSD locations, which shows that surface deflections increased by between four and eleven times along the length of the test section, indicating significant damage in the pavement structure in terms of loss of stiffness. The ratio of final-to-initial deflections is inconsistent across the section, with significantly higher values at one end of the section compared to the other. When the results are considered in conjunction with Figure 2.3, lower deflections (4CL and 6CL) were recorded at the end of the section that had little cracking in the underlying pavement (stiffer pavement), while those with the highest deflections (8CL, 10CL, and 12CL) are over the severely cracked area (weaker pavement).

Deflections and damage rates both increased with increase in load. Figures 3.6 to 3.10 compare the deflection bowls at the same locations at test start, at load change intervals, and at test completion. The same scale is used on all figures, and the increasing deflection over time and with load is clear. The higher deflections at points 8CL, 10CL, and 12CL over the cracked underlying DGAC are obvious as the test progresses.

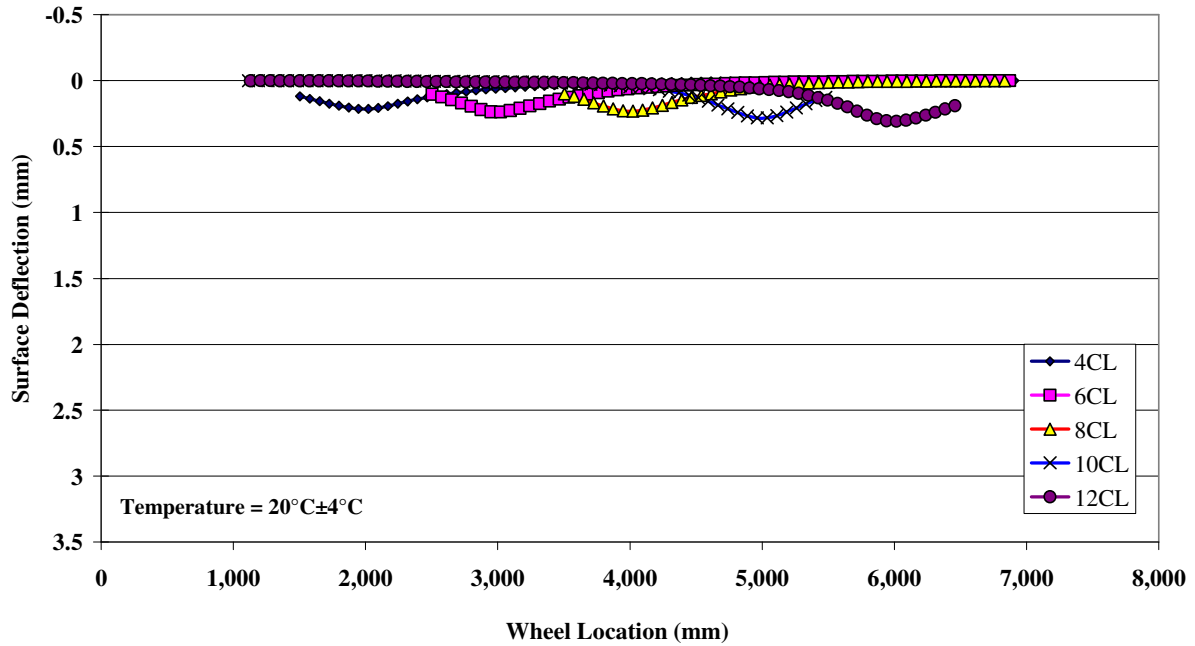


Figure 3.6: RSD deflections at CL locations with 60 kN test load at test start.

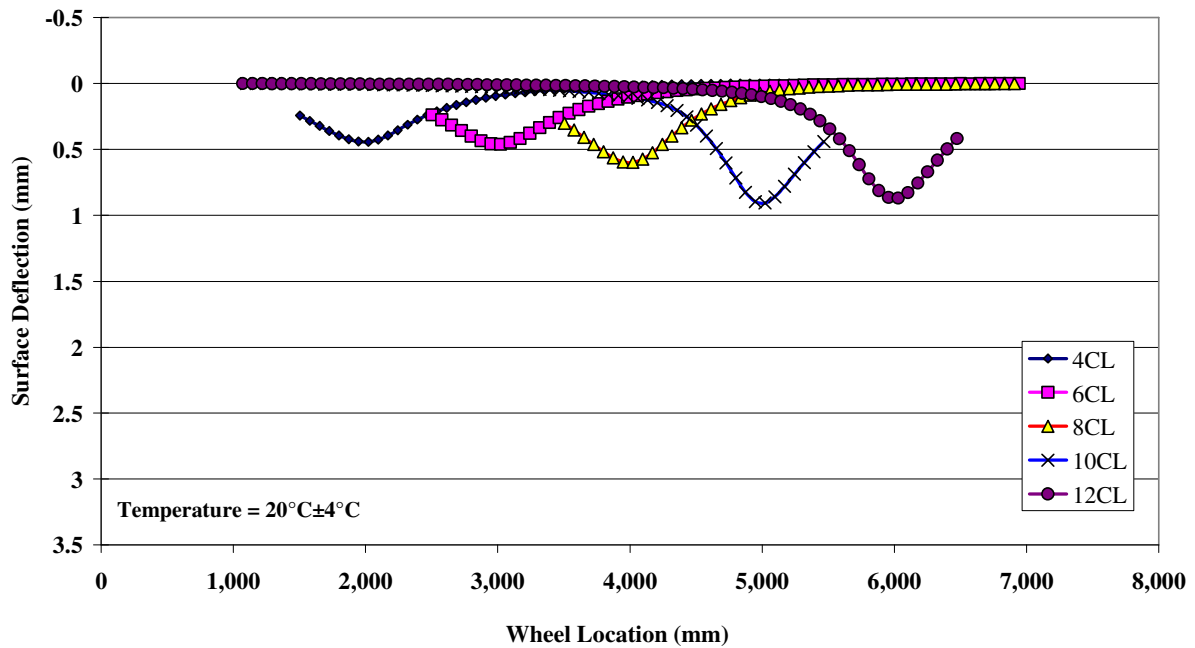


Figure 3.7: RSD deflections at CL locations with 60 kN test load after 215,000 repetitions.

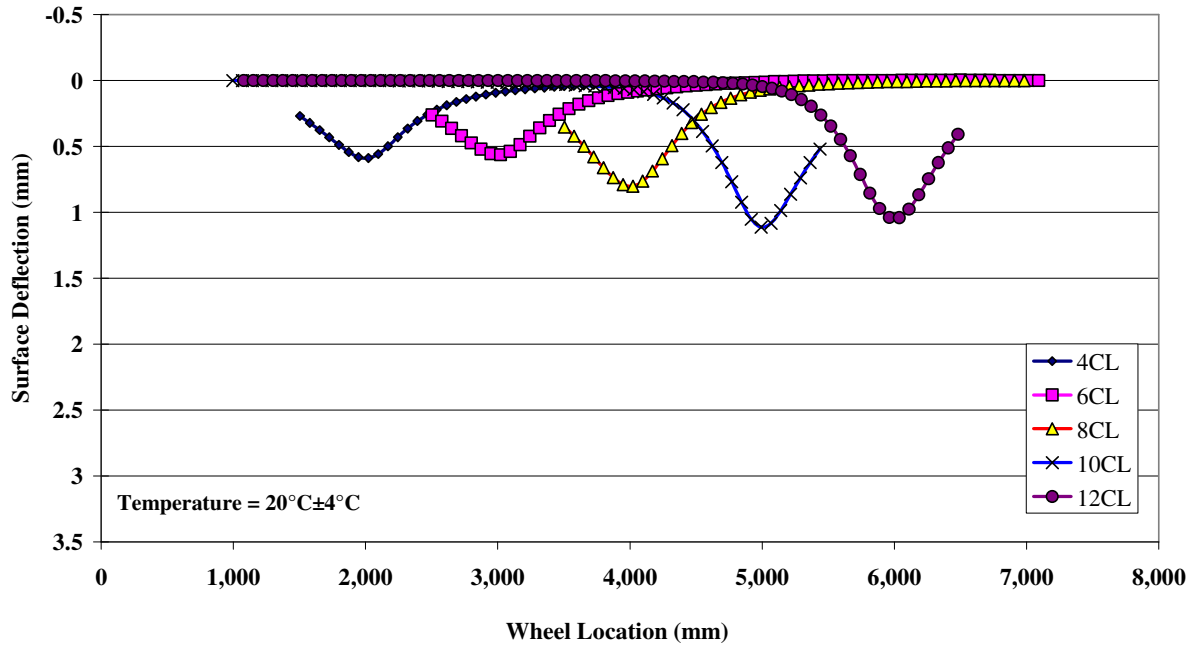


Figure 3.8: RSD deflections at CL locations with 60 kN test load after 417,000 repetitions.

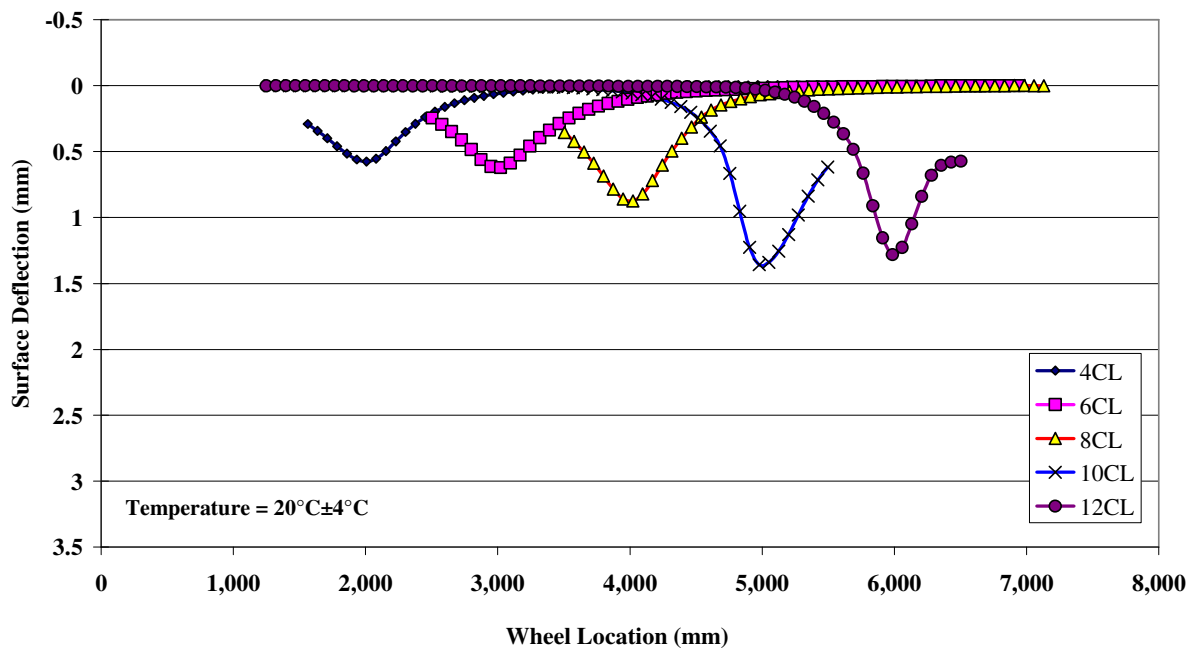


Figure 3.9: RSD deflections at CL locations with 60 kN test load after 1,005,600 repetitions.

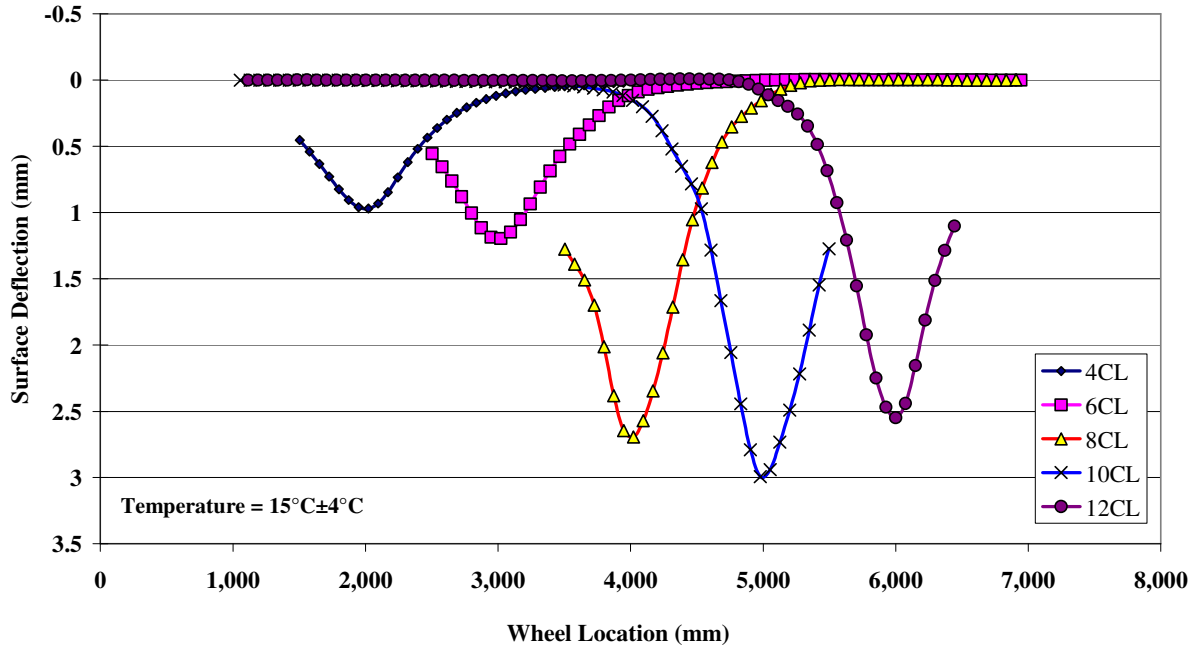


Figure 3.10: RSD deflections at CL locations with 60 kN test load at test completion.

The average 60 kN RSD deflections at centerline and side locations (200 mm from centerline within the trafficked area) are illustrated in Figure 3.11. These deflections are mostly all within 0.2 mm of each other for the first one million repetitions, but after the load increase to 100 kN, deflections along the centerline increase with increasing repetitions, whilst the side deflections remain relatively constant. These results indicate that damage was somewhat greater in the vicinity of the centerline compared to the area away from the centerline where fewer repetitions were applied by the programmed wander of the HVS trafficking pattern.

Figure 3.12 shows the average 60 kN deflection at centerline as well as the averages for measurements taken at the end of the section with more severely cracked DGAC underneath (8CL, 10CL, and 12CL) and the end with less severe cracking (4CL and 6CL). The difference in deflections is clear between the two ends. In Figures 3.11 and 3.12, some sensitivity of RSD deflection to temperature is evident, for example at approximately 100,000 repetitions, 600,000 repetitions, the load change at 1,000,000 repetitions, and at 1,280,000 repetitions. The influence of temperature on deflection will be discussed in the second-level analysis report. The sensitivity of the RSD to a load reduction is evident in the early phase of 80 kN loading.

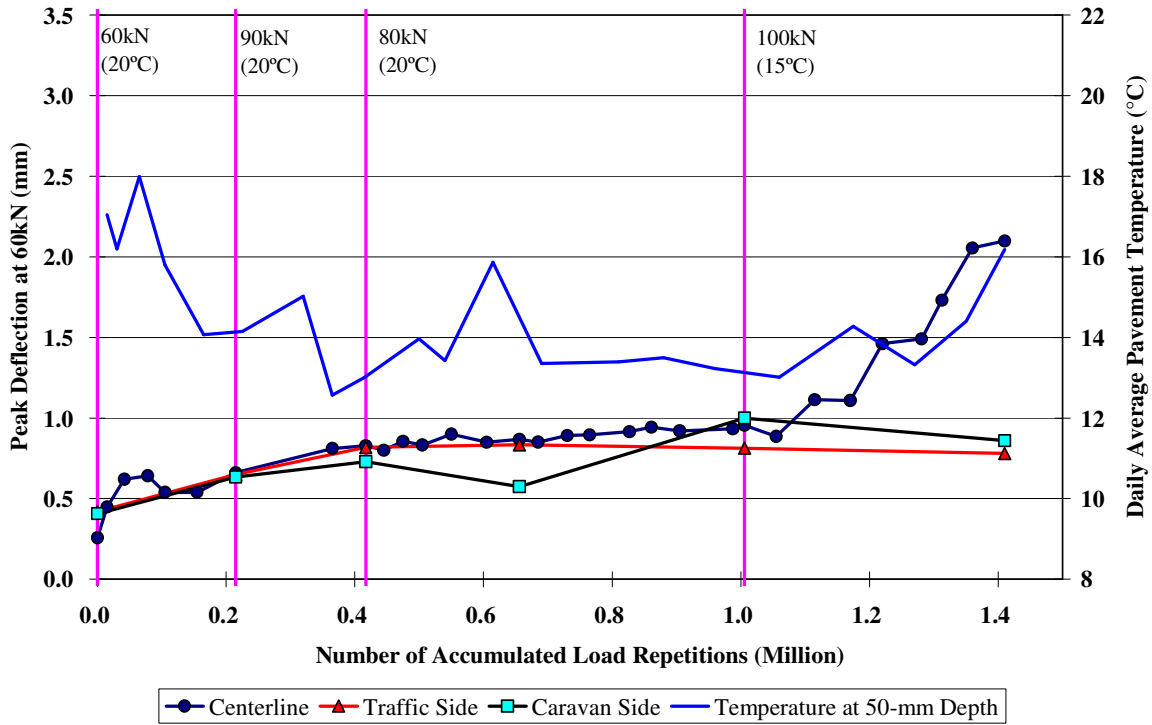


Figure 3.11: Average RSD surface deflections with 60 kN test load (centerline and sides).

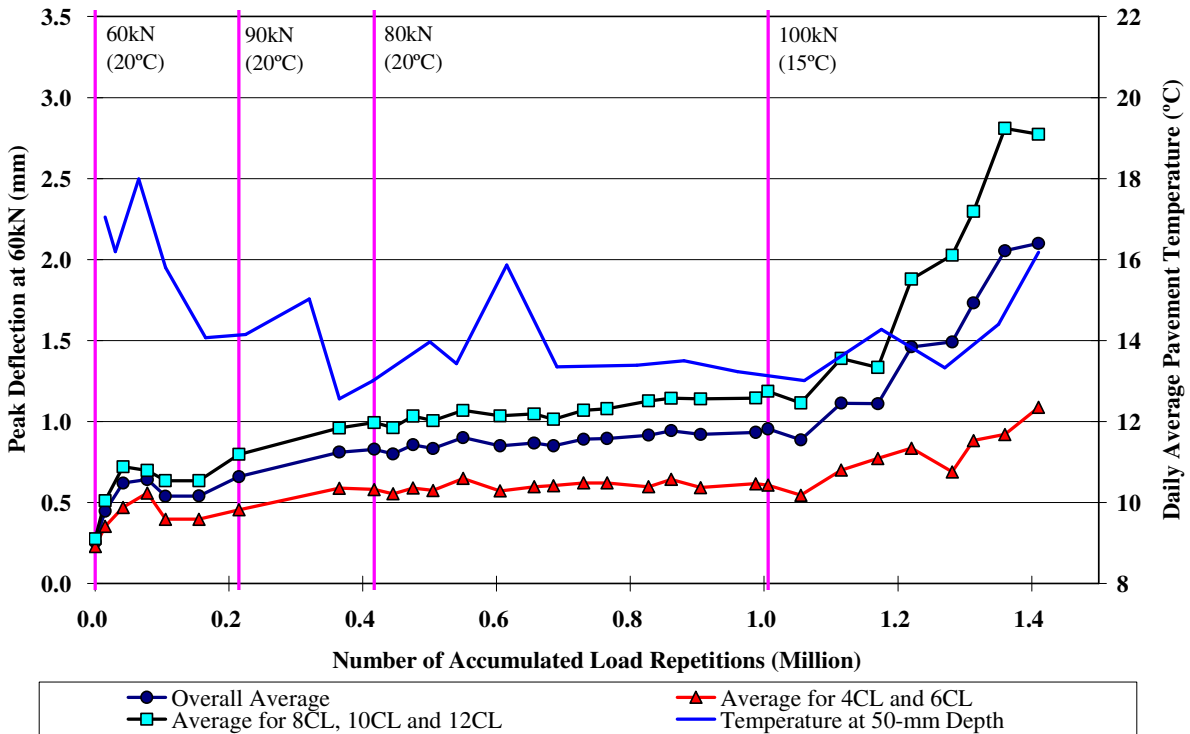


Figure 3.12: Average RSD surface deflections with 60 kN test load (centerline and subsection).

3.3.2 Surface Elastic Deflection Using FWD

FWD testing was conducted on the section before and after HVS trafficking to monitor the changes in layer moduli. Table 3.3 summarizes the date, location, temperatures, and average deflections for the section. Temperatures listed are average temperatures. Recordings from two sensors (1 and 6) and two locations (section centerline and side of section) are shown. Sensor 1 (the sensor directly under the falling weight) provides an indication of the deflection of the composite pavement. Sensor 6 provides an indication of the deflection in the subgrade. Centerline readings show deflection on the trafficked area, while readings from the untrafficked side of the section are used to compare trafficked and untrafficked areas. Figures 3.13 through 3.17 show the FWD deflection measurements recorded on the section (note that scales differ between plots). Backcalculation of these results will be discussed in the second-level analysis report.

Table 3.3: Summary of FWD Measurements

Date	Location	Temperatures (°C)		FWD Deflection at 40 kN (microns) ¹			
				Sensor 1		Sensor 6	
		Air	Surface	Average	Std. Dev.	Average	Std. Dev.
After completion of Section 569RF							
06/10/03	Centerline	N/A	24.2	446	140	55	5
06/10/03	Centerline	N/A	28.8	571	181	60	7
Before start of Section 588RF							
10/19/05	Centerline	14.3	15.9	107	10	38	1
10/19/05	Centerline	19.4	25.8	123	10	40	1
10/19/05	Side ²	14.3	17.1	113	8	44	2
10/19/05	Side	17.9	21.4	132	10	49	3
After completion of Section 588RF							
04/28/06	Centerline	16.0	25.1	371	138	48	5
04/28/06	Centerline	16.4	27.7	377	146	49	4
04/28/06	Side	15.3	27.2	134	12	49	2
04/28/06	Side	16.1	27.8	141	10	49	1

¹ Deflections based on measurements between Stations 3 and 13 inclusive

² Side location is 1.0 m from the test section, representing untrafficked area

Figure 3.13 shows the effect of damage on the pavement over the course of the experiment. It should be noted that there appears to be a discrepancy in the Station Numbers for the measurements taken after completion of HVS testing (April 28, 2006) compared to previous measurements. If each data point is shifted by two stations, a more realistic trend is observed. Deflection measured on Section 569RF prior to placing the overlay was relatively high, especially in the area of significant cracking. Placement of the overlay considerably reduced the deflection. However, considerable damage was again caused by the HVS trafficking, with higher damage recorded after the test on parts of the section (Stations 8 through 13) when compared to that after completion of testing on Section 569RF. The overlay provided some structural improvement over the area with less severe cracking (Stations 3 through 7). The figure also shows that deflections were influenced by temperature, with slightly lower deflections measured in the

morning (lower temperature) compared to those measured in the afternoon (higher temperature) at the end of the test.

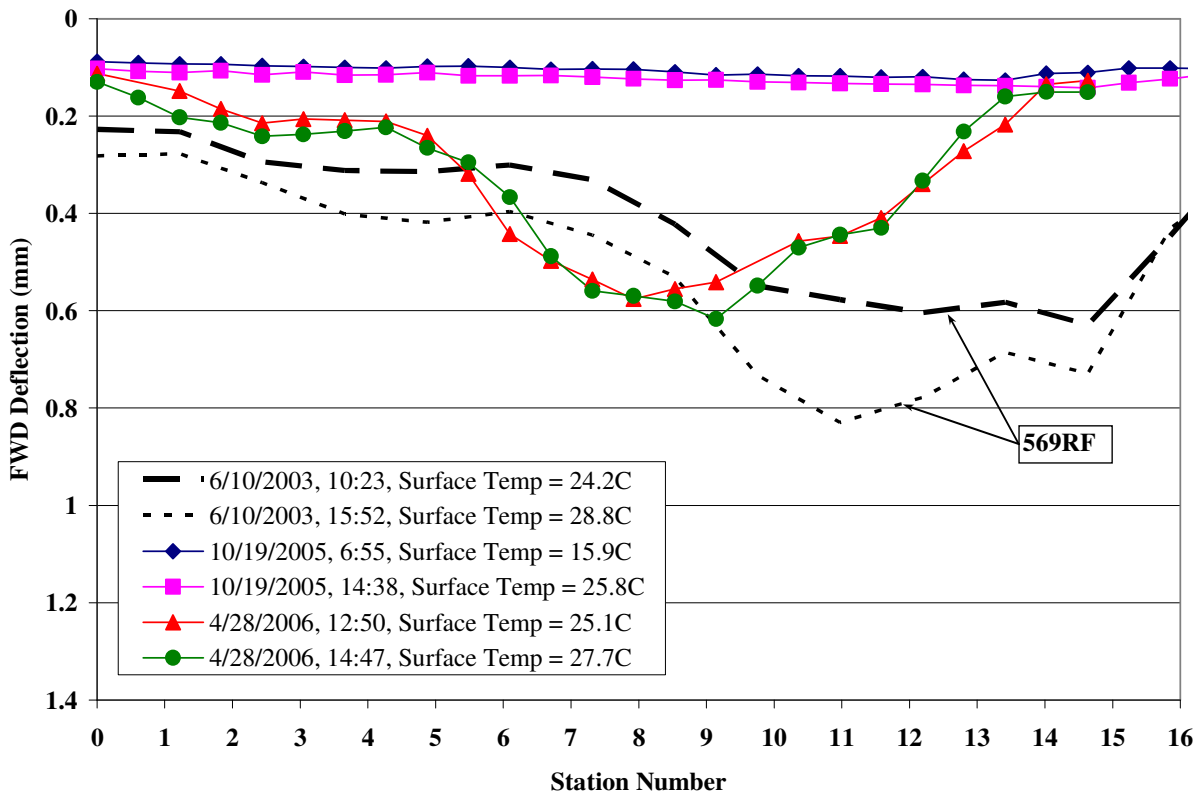


Figure 3.13: Composite pavement stiffness (FWD Sensor 1) on section centerline.

Figure 3.14 shows deflections in the subgrade before and after the test. These measurements indicate that there was no significant change (0.02 mm) during the course of the experiment, and that the overlay provided only minor structural improvement to the overall pavement structure in terms of protection of the subgrade immediately after the overlay was placed. It appears that the subgrade was less stiff at the end of the section that had more cracking in the underlying DGAC (Stations 8 through 13). The slight increase in deflection on completion of the test could be attributed to moisture in the subgrade and/or increased deflections in the upper layers.

Figures 3.15 and 3.16 show FWD deflections taken along the side of the HVS test section but outside the trafficked area (i.e., the area tested did not have traffic damage). These figures can be used to understand the influence of environmental conditions on the performance of the section. The figures show very little change over the course of the experiment. The temperature difference between the two measurements was also marginal and hence little influence of this parameter on deflection was noted.

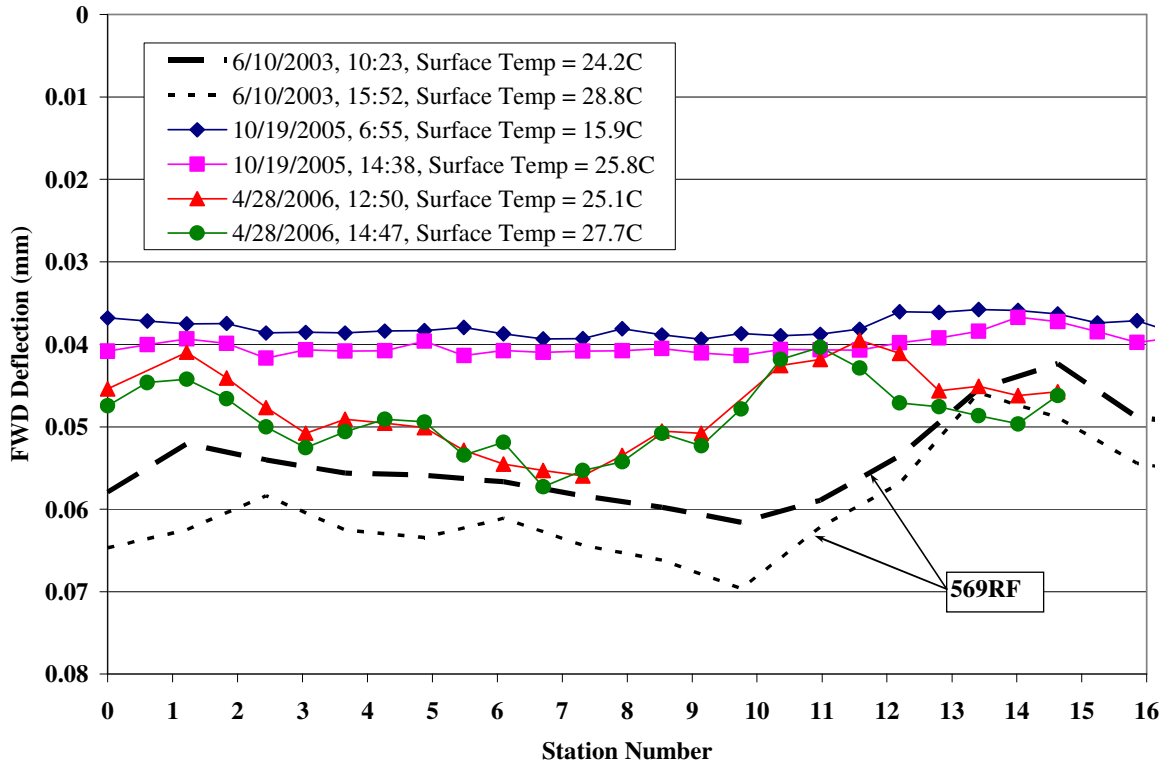


Figure 3.14: Subgrade pavement stiffness (FWD Sensor 6) on section centerline.

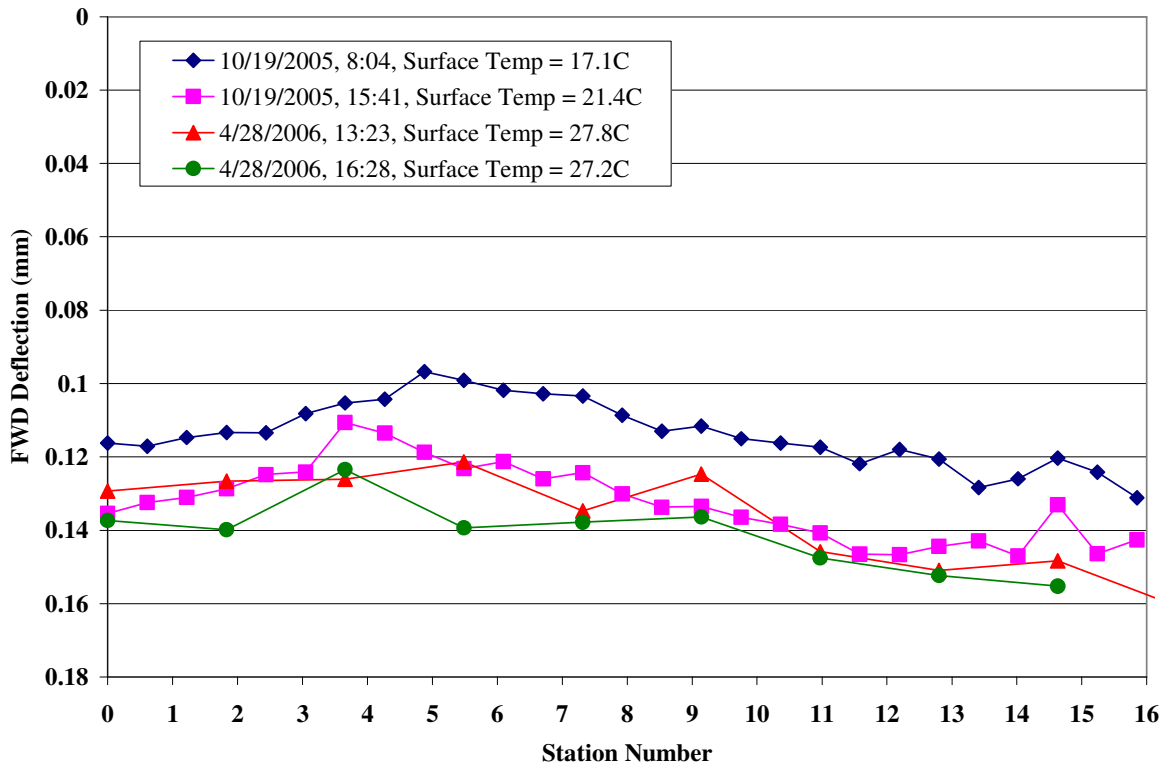


Figure 3.15: Composite pavement stiffness (FWD Sensor 1) outside trafficked area.

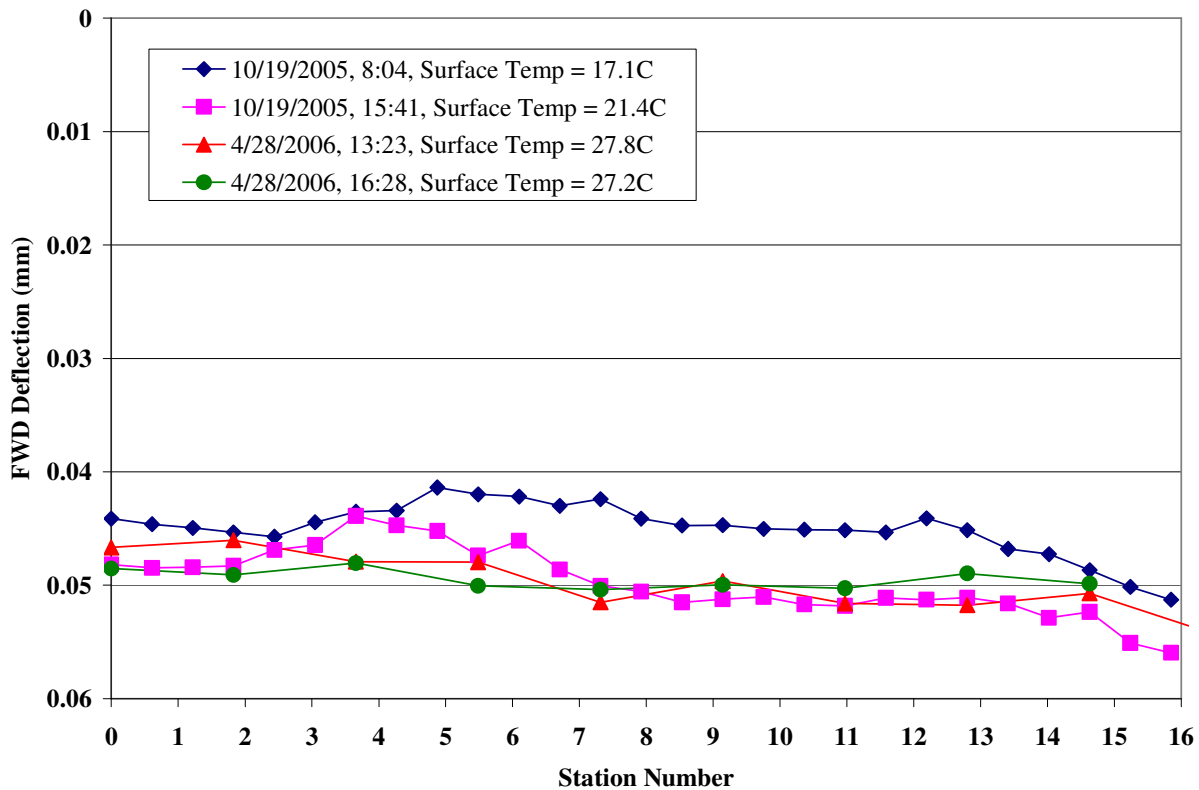


Figure 3.16: Subgrade pavement stiffness (FWD Sensor 6) outside trafficked area.

3.3.3 In-Depth Elastic Deflection

The schedule of MDD measurements with various test loads is listed in Table 2.2. As shown in the table, problems were experienced with the MDD linear variable displacement transducers (LVDT), which resulted in questionable data being collected. These problems were attributed to very wet conditions in the lower layers of the pavement and subgrade, which influenced the anchor points of the MDD stack. No in-depth deflection data will thus be discussed in this report.

Although robust and proven, the LVDTs are delicate instruments and can not be repaired once installed in the pavement.

3.4. Permanent Deformation

Permanent deformation at the pavement surface (rutting) was monitored with the Laser Profilometer and at various depths within the pavement with three Multi-depth Deflectometers (MDDs). Only Laser Profilometer measurements are discussed below. In-depth deformation will be discussed in the second-level analysis report after test pits have been excavated.

3.4.1 Permanent Surface Deformation (Rutting)

Deformation and rutting on HVS tests are usually analyzed using two definitions, namely maximum rut depth and maximum deformation (4), as illustrated in Figure 3.17. The Laser Profilometer is used to measure these distresses and provides sufficient information to evaluate the evolution of permanent surface deformation of the entire test section at various loading stages.

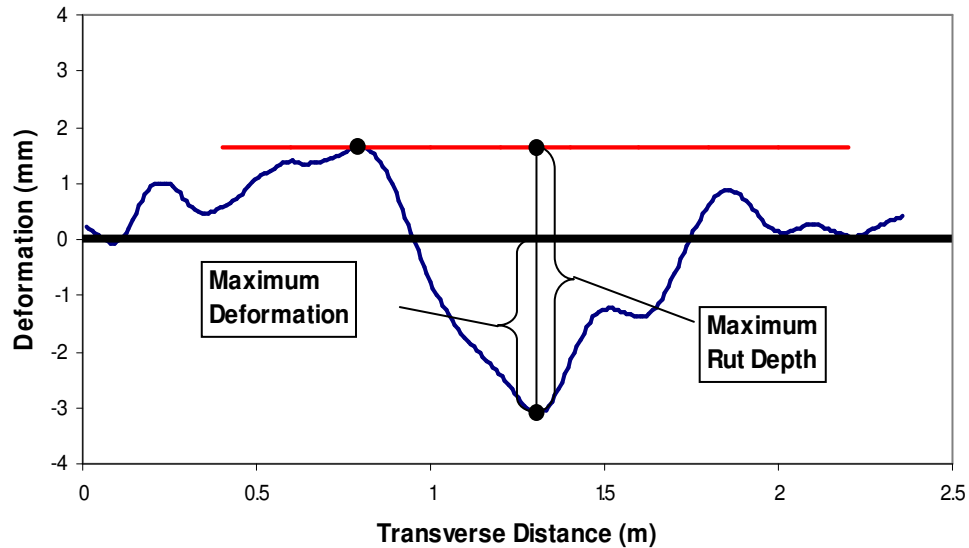


Figure 3.17: Illustration of maximum rut depth and maximum deformation of a leveled profile.

Figure 3.18 shows the average transverse cross section measured with the Profilometer at various stages of the test. This plot clearly shows the increase in rutting and deformation over the duration of the test.

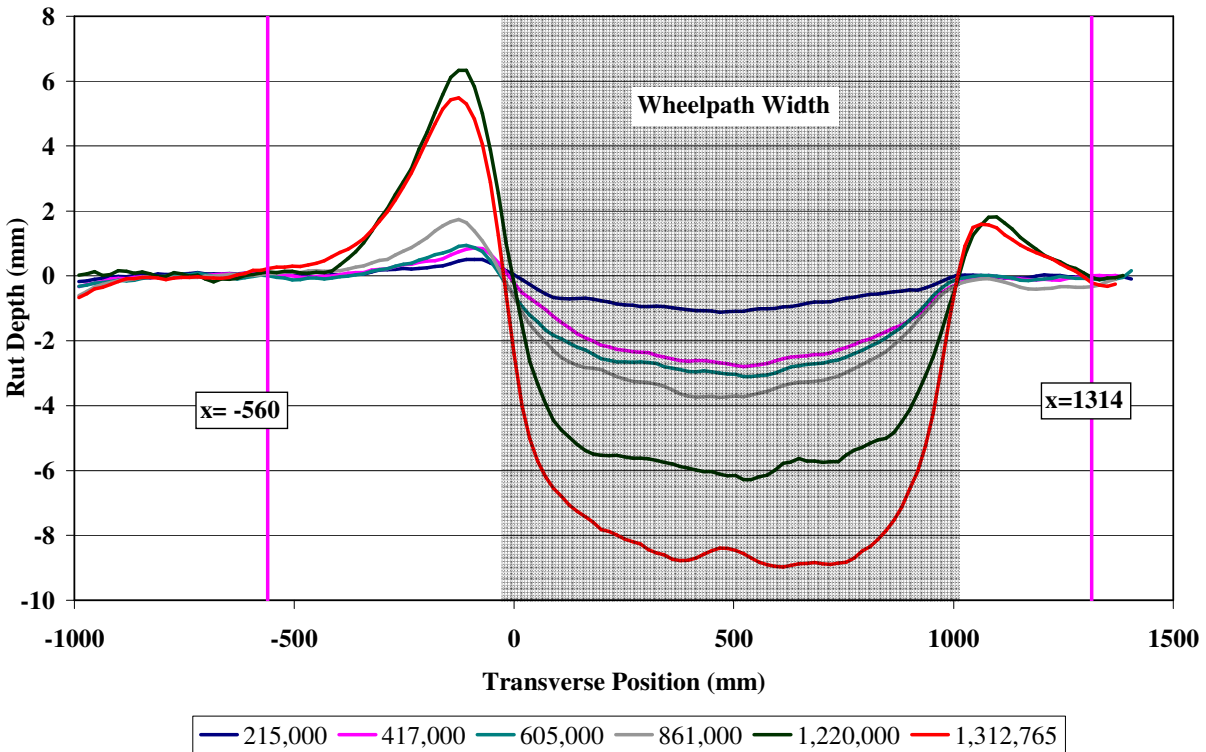


Figure 3.18: Profilometer cross section at various load repetitions.

During HVS testing, rutting usually occurs at a high rate initially and then typically diminishes as trafficking progresses until reaching a steady state. If the load level is subsequently increased, the pavement will normally undergo another phase of rapid rutting development until a steady phase for that new load level is reached. This initial phase is referred to as the “embedment” phase. Figures 3.19 and 3.20 show the development of permanent deformation (maximum deformation and maximum rut, respectively) with load repetitions as determined by the Laser Profilometer for the test section with an embedment phase apparent at the beginning of the experiment and at the 90 kN and 100 kN load changes. Rut development is relatively constant until the 100 kN load change, after which it increases at a much higher rate. Error bars on the average reading indicate variation along the length of the section. The figures also show average maximum deformation and average maximum rut for Stations 3 to 7 and 8 to 13. Stations 8 to 13 are over the end of the section where the underlying DGAC was significantly cracked, while Stations 3 to 7 are over the end with less severe cracking. The figures show that deformation and rut are considerably higher over the significantly cracked section.

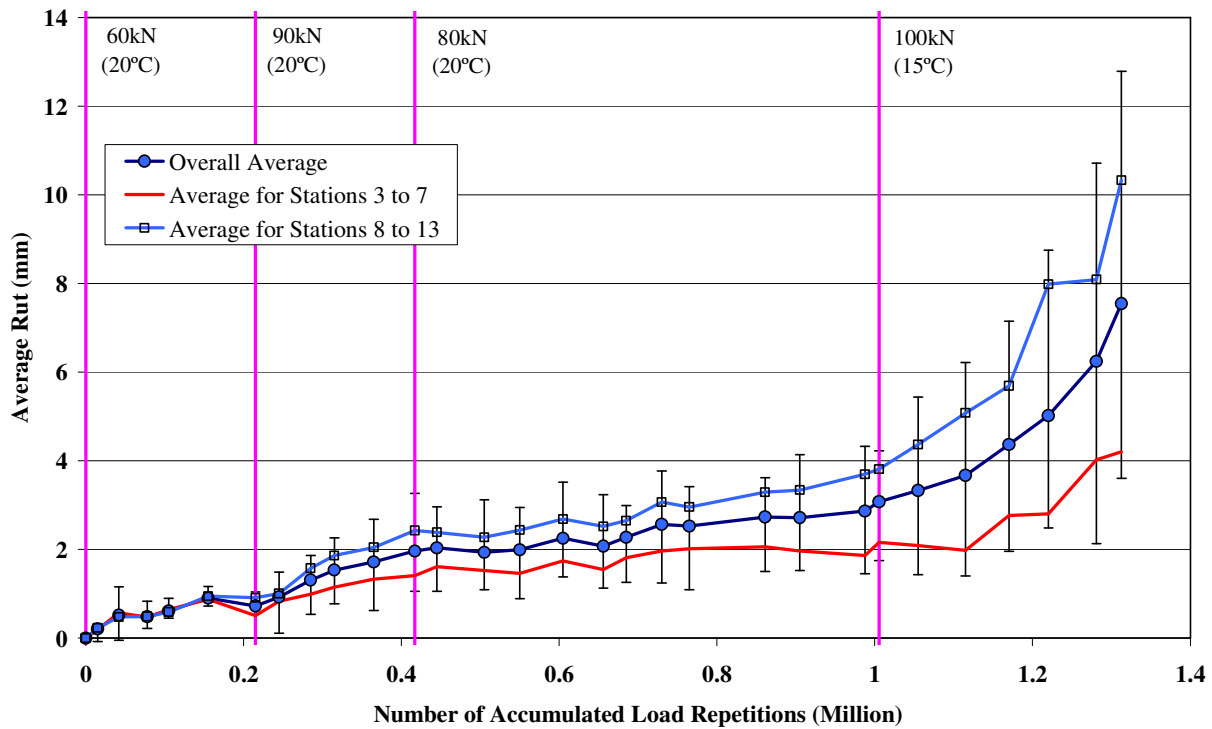


Figure 3.19: Average maximum deformation determined from Laser Profilometer data.

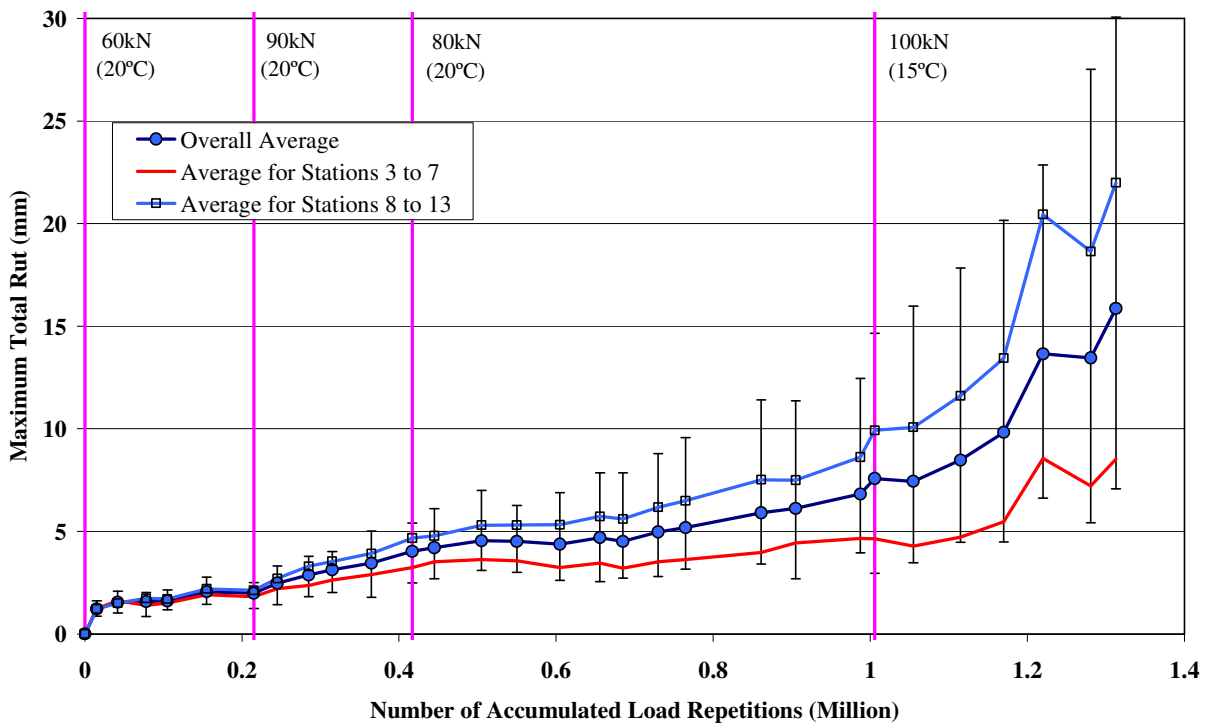


Figure 3.20: Average maximum rut determined from Laser Profilometer data.

Figure 3.21 shows a contour plot of the pavement surface after the first load change at 215,000 repetitions, when the second embedment phase started. Figures 3.22 through 3.25 show contour plots of the rutting progression on the surface at 417,000 repetitions (second load change), 860,000 repetitions (mid-80 kN loading phase), one million (100 kN load change), and on completion of the test. The increase in rutting between the 100 kN load change and test completion is clear in Figure 3.25 when compared to Figure 3.23.

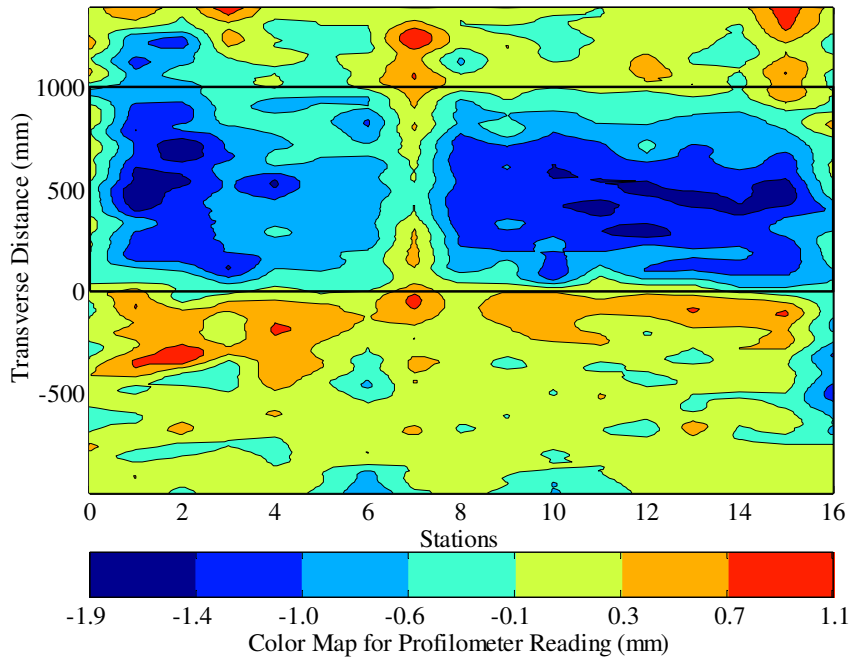


Figure 3.21: Contour plot of permanent deformation after 215,000 repetitions.

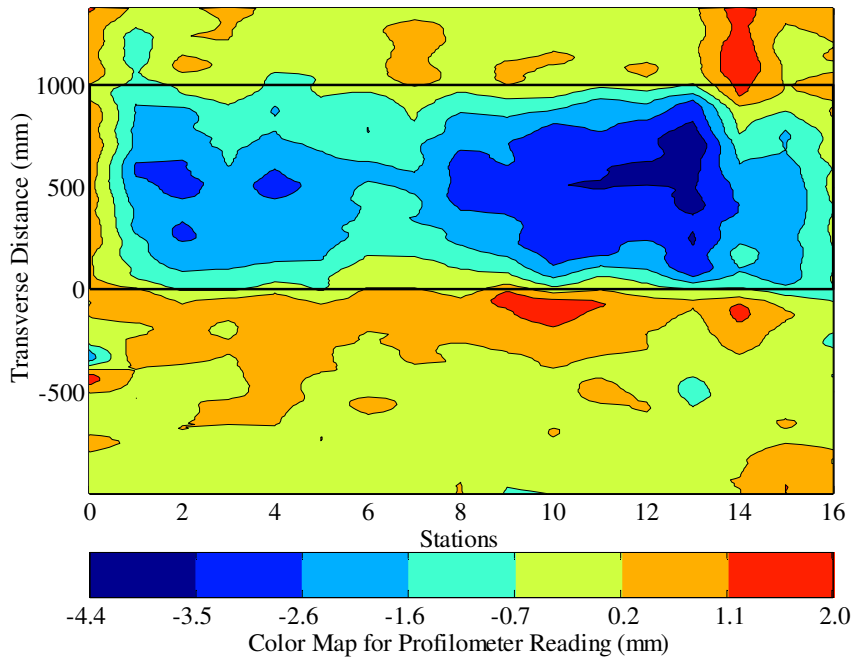


Figure 3.22: Contour plot of permanent deformation after 417,000 repetitions.

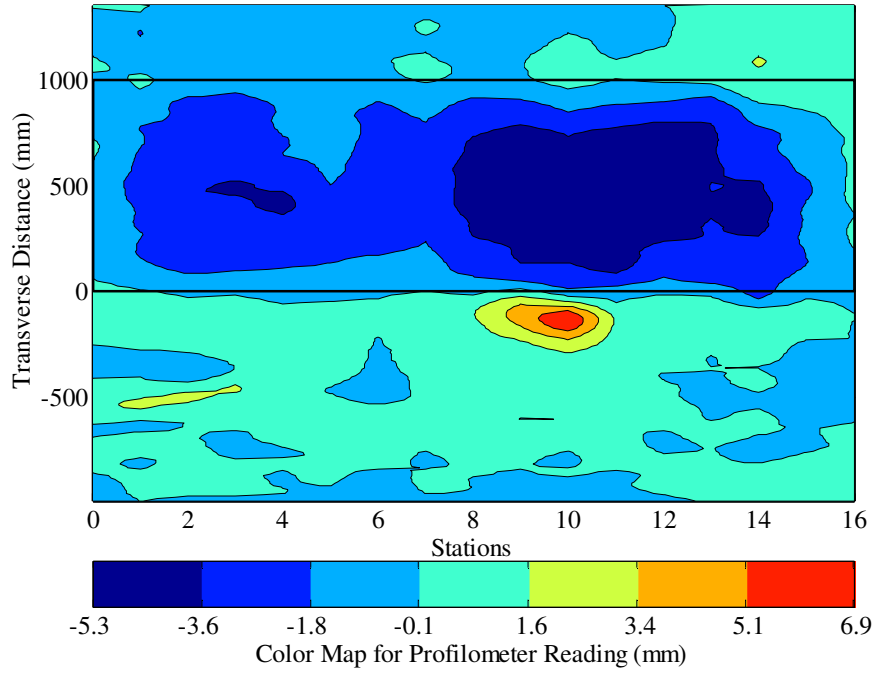


Figure 3.23: Contour plot of permanent deformation after 861,000 repetitions.

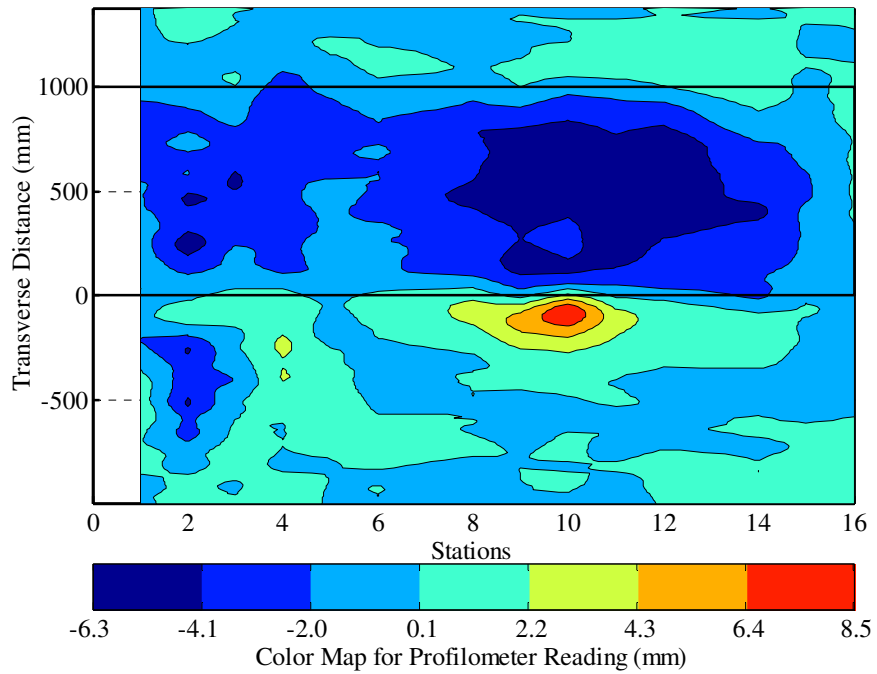


Figure 3.24: Contour plot of permanent deformation after 1,006,000 repetitions.

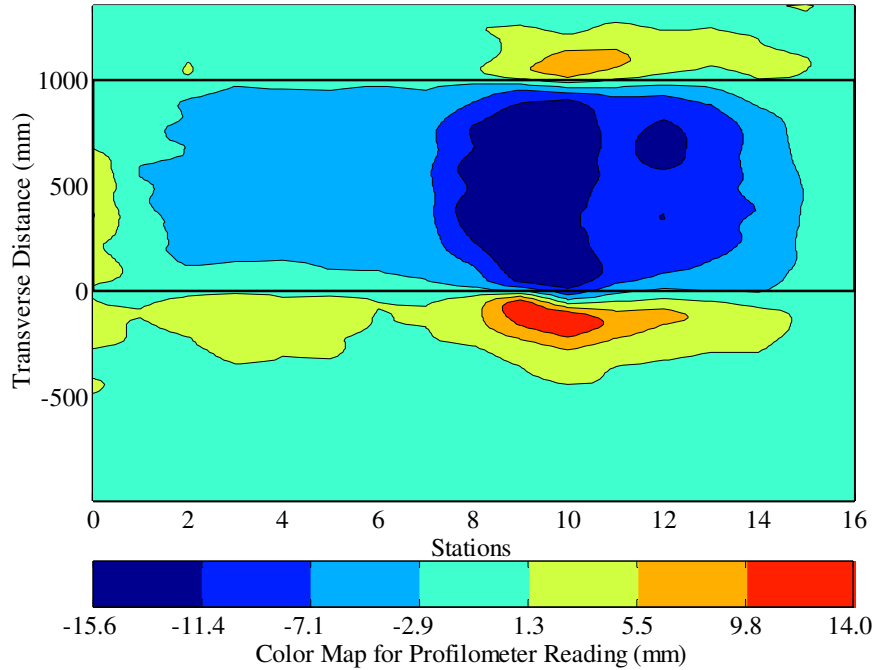


Figure 3.25: Contour plot of permanent deformation after test completion.

After completion of trafficking (1.41 million load repetitions), the average maximum deformation and the average maximum rut depth were 8.8 mm and 15.9 mm, respectively. The maximum rut depth measured on the section was 30.0 mm. Although the test plan indicated that HVS trafficking should be halted when the average maximum rut depth had exceeded 12.5 mm (approximately 1.2 million repetitions), testing was continued to determine whether cracking would eventually spread to the remainder of the test section. The final surface rutting pattern of the overlay generally corresponds with the fatigue cracking pattern of the cracked DGAC layer as shown in Figure 3.26, with the deepest rut occurring on that half of the section with the highest density of cracking in the underlying layer.

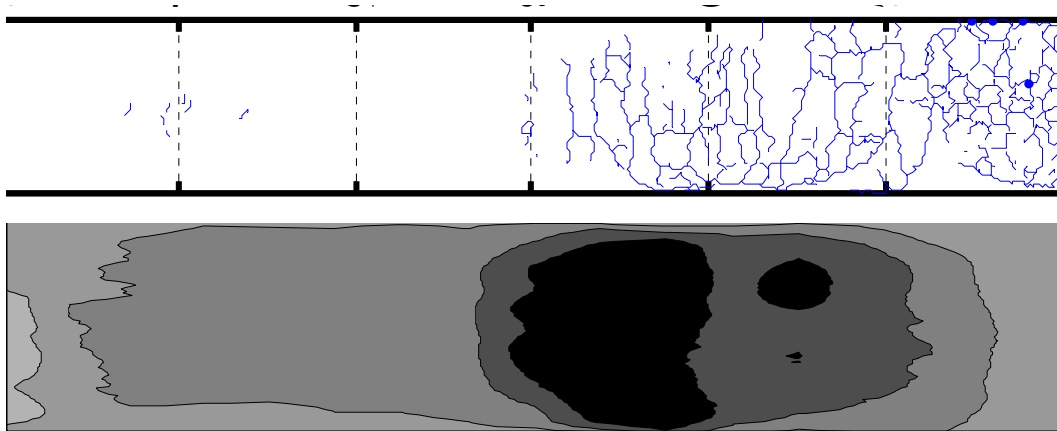


Figure 3.26: Comparison of Phase I cracking pattern and Phase II rutting at test completion.

3.4.2 Permanent In-Depth Deformation

The accumulation of vertical deformation at various depths in the pavement is measured with MDD linear variable displacement transducer (LVDT) modules during the course of HVS testing. Permanent deformation measured by each LVDT is the total permanent deformation of the pavement between the anchoring depth (3.0 m) and the depth of the module. Accordingly, LVDT modules in the upper part of the pavement typically measure larger permanent deformation than those in the lower part. The difference in measured permanent deformation between two LVDT modules represents the permanent deformation accumulated in the layers between those two modules. This is known as differential permanent deformation. Module locations for Section 588RF are shown in Figure 2.6 and are listed below.

- 186 mm: near the bottom of the cracked DGAC layer;
- 355 mm: in the middle of the aggregate base layer;
- 523 mm: at the bottom of the aggregate base layer, and
- 823 mm: 300 mm below the top of the subgrade.

A module was not installed on the surface of the AR4000-D overlay due to thickness constraints.

Problems were experienced with the MDD linear variable displacement transducers (LVDT) during the course of the experiment, which resulted in questionable data being collected. These problems were attributed to very wet conditions in the lower layers of the pavement and subgrade, which influenced the anchor points of the MDD stack. No in-depth permanent deformation data will thus be discussed in this report.

3.5. Visual Inspection

Fatigue distress in an asphalt concrete pavement manifests itself in the form of surface cracks. Since this study centered on fatigue cracking and the ability of the overlay to limit reflective cracking from the underlying layer, crack monitoring was an essential component of the data collection program. This entails:

- Visual inspections of the test section and marking of visible cracks;
- Photographic documentation of the marked cracks;
- Correction of the photos for camera angle;
- Digitization of the photos;
- Calculation of the crack length using *Optimas*TM software, and
- Presentation of the cracking in terms of crack length per area of pavement.

Regular crack inspections were made from the time that the first crack was detected through to the end of testing. The first cracks appeared around the MDD top caps at Stations 4 and 8 and at various positions between Stations 8 and 15 after about 510,000 repetitions. Thereafter, cracks continued to appear throughout the remainder of the trafficking, predominantly between Stations 7 and 15. The observed cracks varied in width between 1.0 mm and 3.0 mm. The cracks did not spall, but some increased in width during testing. Some pumping was evident in the latter stages of the test after prolonged rainfall. Most cracking was in the form of transverse and alligator cracks as with the underlying layer. At the end of testing, 197 cracks were identified with a total length of 54.62 m and variable spacing. This equates to a crack density of 9.1 m/m^2 , which significantly exceeds the failure criterion of 2.5 m/m^2 set for the experiment, reached after approximately 900,000 repetitions. This cracking was predominantly between Stations 8 and 15 (Figure 3.27) and therefore testing was continued to determine whether cracking would eventually spread to the remainder of the test section. Figure 3.28 shows a photograph taken of the surface between Stations 10 and 12 on completion of testing. Crack density of the underlying DGAC layer was 6.05 m/m^2 after approximately 217,000 repetitions. On Section 588RF, this crack density was reached after approximately one million repetitions.

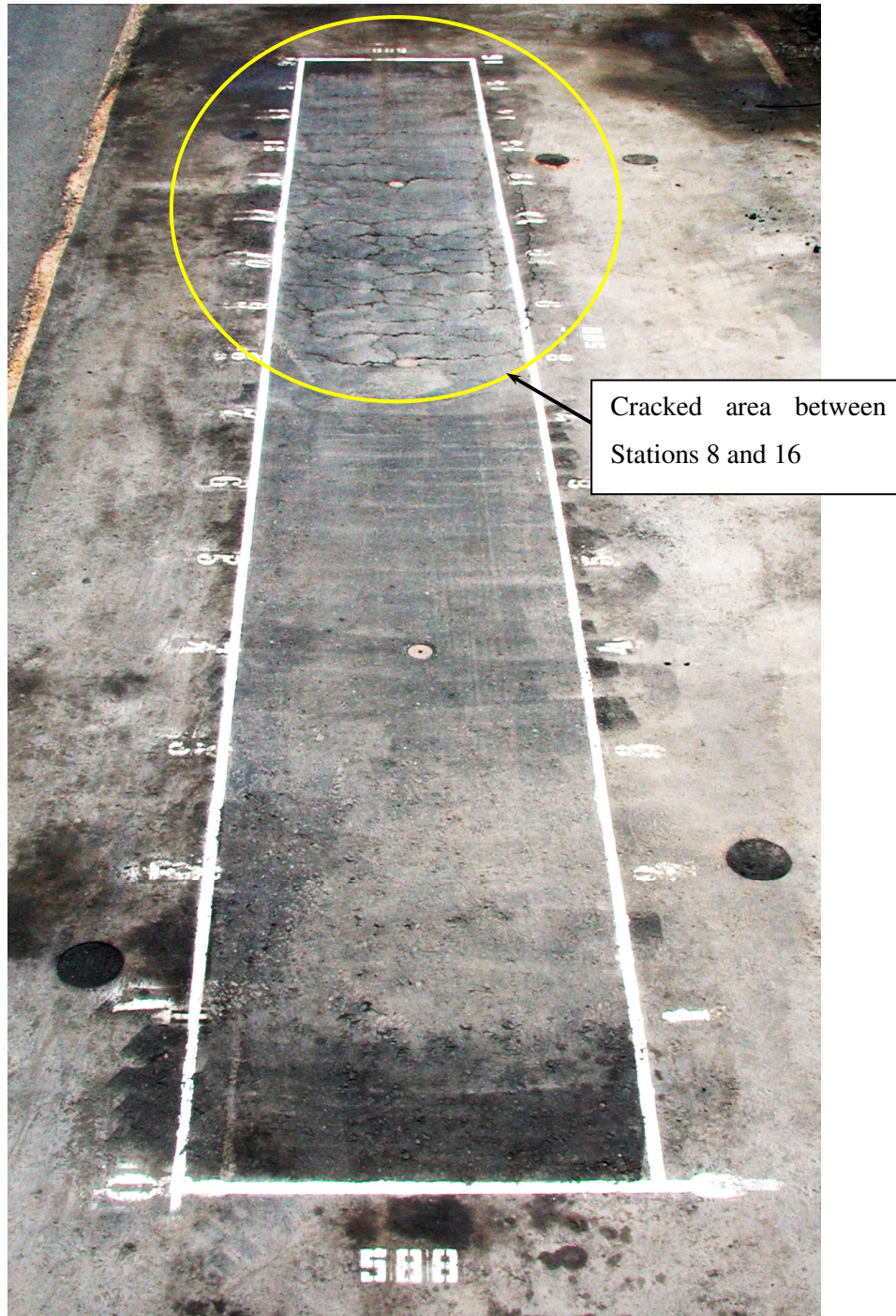


Figure 3.27: Photograph of Section 588RF showing cracks in one half of the section.



Figure 3.28: Surface cracks marked with crayon between Stations 10 and 12 at end of test.

Figures 3.29 and 3.30 illustrate the sequence of surface crack patterns at various load applications. As seen in these figures, cracking was predominantly transverse between 500,000 and one million repetitions. After the 100 kN load change, the rate of cracking appears to accelerate and the pattern changes to that of alligator cracking.

Figure 3.31 compares the cracking on completion of testing on Section 588RF with that on the underlying Section 569RF. The cracks do not match exactly, but provide an indication of reflection from the underlying layer. The areas of severe cracking in the underlying layer are matched in the overlay, specifically between Stations 8 and 13. The reasons for this cracking behavior will only be fully understood after completion of the forensic investigation, when test pits in both areas will be excavated.

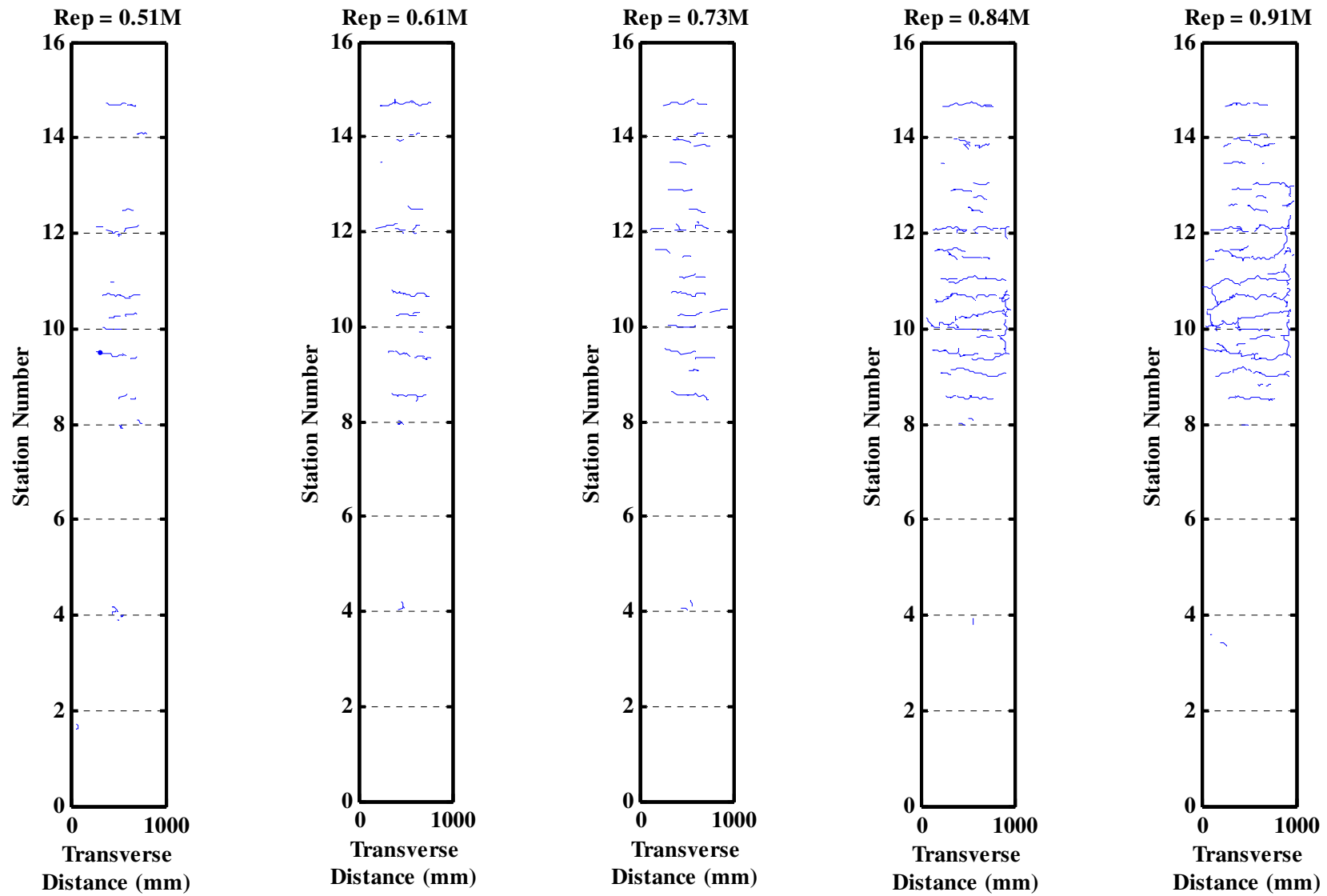


Figure 3.29: Crack development between 510,000 and 910,000 repetitions.

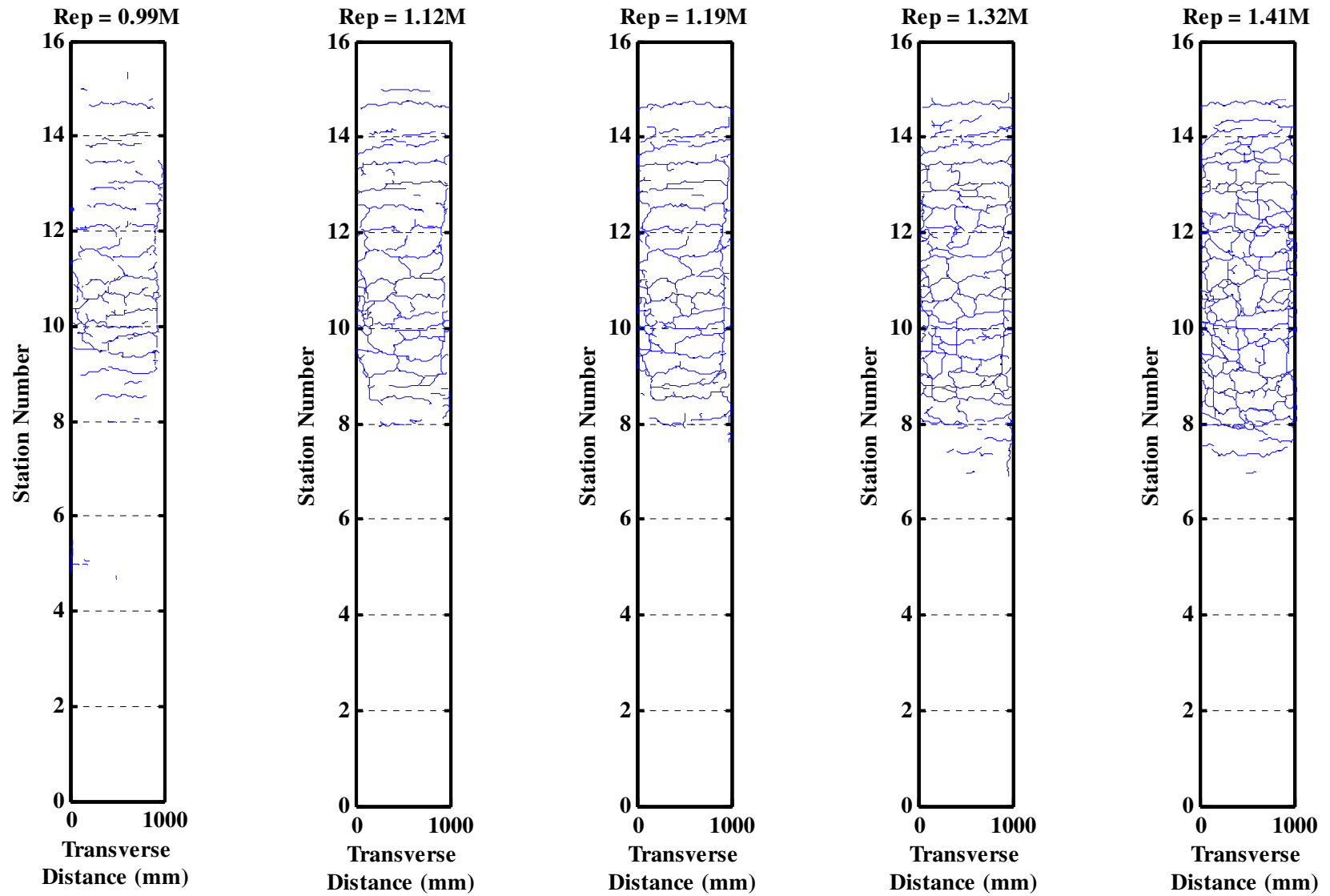


Figure 3.30: Crack development between 990,000 repetitions and test completion.

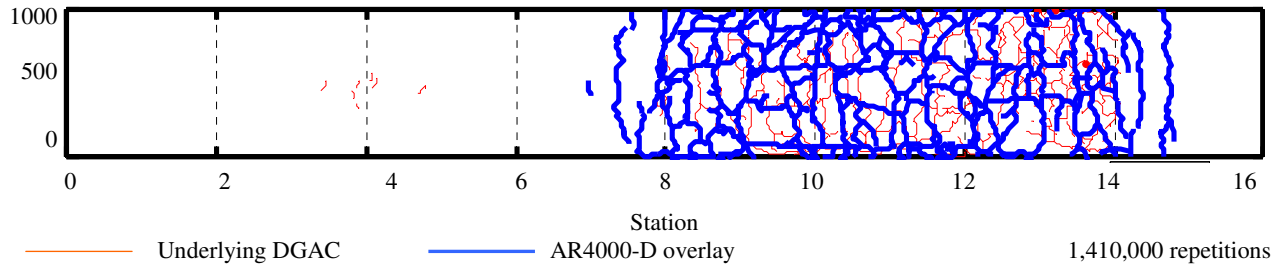


Figure 3.31: Cracking pattern comparison between underlying layer and overlay.

Further analysis of the cracks indicated that the crack accumulation history can be fitted reasonably well with the following exponential functions. Equation 3.1 predicts the crack density calculated over the full trafficked section (i.e., 6.0 m²), while Equation 3.2 predicts crack density over the actual area that cracked (ie 3.7 m²). Results are plotted in Figure 3.32.

Full trafficked Section (6.0 m²): $CD = 0.1086e^{3.3075N}$...Equation 3.1

Cracked Section only (3.7 m²): $CD = 0.1761e^{3.3075N}$...Equation 3.2

Where: CD is the crack density in m/m²
 N is the number of accumulated load repetitions in millions.

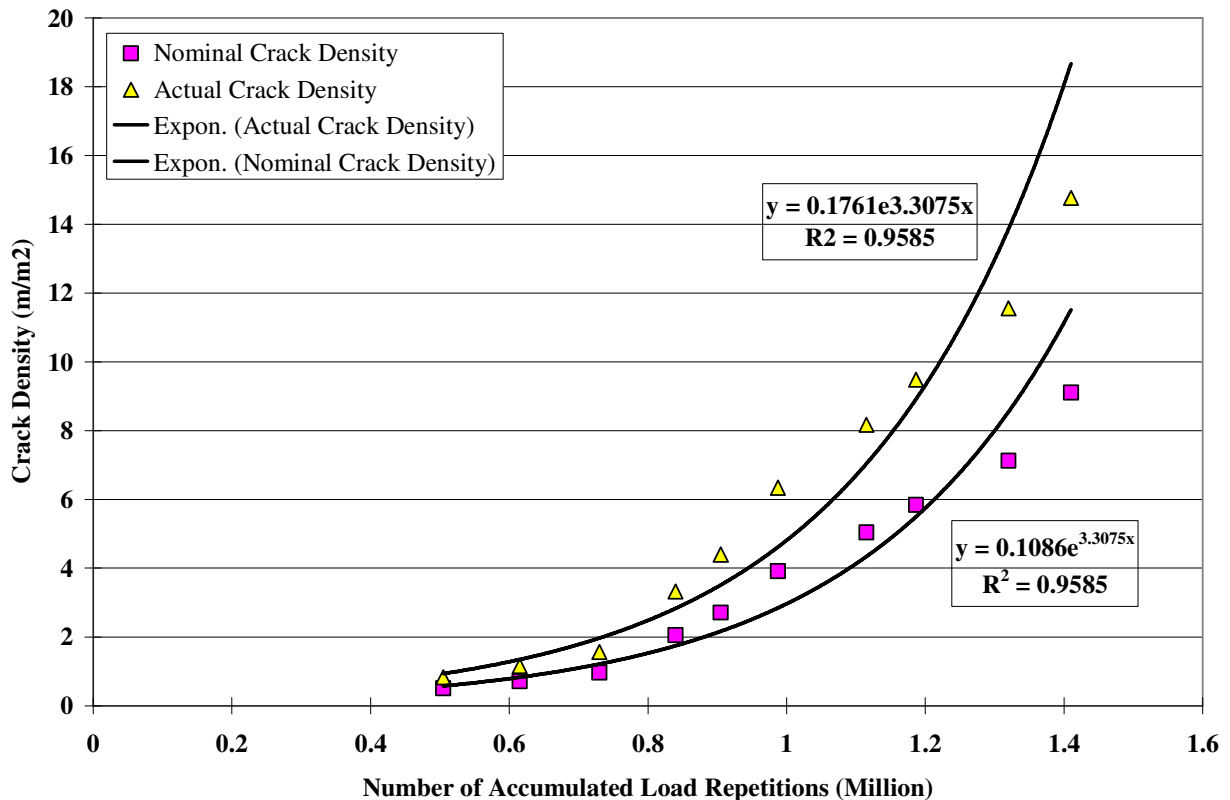


Figure 3.32: Crack accumulation with trafficking.

3.6. Forensic Evaluation

A forensic evaluation (coring and test pit) can only be undertaken when HVS testing on all of the six sections has been completed. Results of the forensic evaluation will be discussed in a second-level analysis report on completion of the tests.

3.7. Second-Level Analysis

A second-level analysis report will be prepared on completion of all HVS testing and a forensic evaluation. This report will include:

- Actual layer thicknesses;
- Backcalculation of moduli from RSD, MDD, and FWD measurements;
- Verification of data collected from in-depth measurements with visual observations from test pits;
- Comparison of performance between test sections;
- Comparisons of HVS test results with laboratory test results, and
- Recommendations.

4. CONCLUSIONS

This First-level Report is the fourth in a series of studies detailing the results of HVS testing being performed to validate Caltrans overlay strategies for the rehabilitation of cracked asphalt concrete. It describes the results of the fourth HVS reflective cracking testing section, designated 588RF, carried out on a 90 mm (3.5 in) full-thickness AR4000-D overlay, included in the experiment as a control for performance comparison purposes. Other overlays that will be tested during the course of the experiment include

- Half-thickness (45 mm) MB4 gap-graded overlay (45 mm MB4-G);
- Full-thickness (90 mm) MB4 gap-graded overlay (90 mm MB4-G);
- Half-thickness (45 mm) MB4 gap-graded overlay with minimum 15 percent recycled tire rubber (MB15-G);
- Half-thickness (45 mm) MAC15TR gap-graded overlay with minimum 15 percent recycled tire rubber (MAC15-G), and
- Half-thickness rubberized asphalt concrete gap graded overlay (RAC-G) overlay, included as a control for performance comparison purposes.

The pavement was designed according to the Caltrans Highway Design Manual Chapter 600 using the computer program *NEWCON90*. Design thickness was based on a subgrade R-value of 5 and a Traffic Index of 7 (~121,000 ESALs). The overlay thickness was determined according to Caltrans Test Method (CTM) 356 using Falling Weight Deflectometer (FWD) deflections.

HVS trafficking on the section commenced on November 2, 2005, and was completed on April 11, 2006. A temperature chamber was used to maintain the pavement temperature at $20^{\circ}\text{C}\pm 4^{\circ}\text{C}$ ($68^{\circ}\text{F}\pm 7^{\circ}\text{F}$) for the first one million repetitions, then at $15^{\circ}\text{C}\pm 4^{\circ}\text{C}$ ($59^{\circ}\text{F}\pm 7^{\circ}\text{F}$) for the remainder of the test. A total of 1,410,000 load repetitions (tire pressure of 720 kPa [104 psi], and bi-directional trafficking pattern with wander) were applied during this period consisting of:

- 215,000 repetitions of a 60 kN (13,500 lb) load;
- 202,000 repetitions of a 90 kN (20,250 lb) load;
- 588,600 repetitions of an 80 kN (18,000 lb) load, and
- 404,400 repetitions of a 100 kN (22,500 lb) load.

This loading equates to approximately 37 million equivalent standard axles, using the Caltrans conversion of $(\text{axle load}/18000)^{4.2}$, which in turn equates to a Traffic Index of 13.8.

Testing was interrupted during breakdowns between November 7 and November 15, 2005, and March 2 and March 6, 2006 when the cumulative traffic repetitions were approximately 15,000 and 861,000 respectively, and during the holiday shutdown between December 16, 2005 and January 8, 2006, when the repetition count was approximately 315,000.

Laboratory fatigue and shear studies have been conducted in parallel with HVS testing. Results of these studies will be detailed in separate reports. Comparison of the laboratory and test section performance, including the results of a forensic investigation to be conducted when all testing is complete, will be discussed in a second-level report once the data from each of the studies have been collected.

Findings and observations based on the data collected during this HVS study include:

- Cracking was first observed after approximately 510,000 repetitions. On completion of testing, the surface crack density was 9.1 m/m^2 (2.77 ft/ft^2), with cracking occurring predominantly on one half of the section (Stations 8 to 15). The surface crack density reached 2.5 m/m^2 (0.76 ft/ft^2), the failure criterion set for the experiment, after about 900,000 load repetitions, but trafficking was continued to determine whether cracking would eventually spread to the remainder of the test section. Cracking on the overlay was predominantly transverse up until the 100 kN (22,500 lb) load change. Thereafter, an alligator cracking pattern was observed, similar to that on the underlying layer. The crack patterns of the two layers did not match exactly, however, the areas of most severe cracking corresponded. Test pit investigations will provide insights into what influenced the cracking patterns observed. FWD testing revealed a weaker structure under the area of most severe cracking.
- The average maximum rut depth and average maximum deformation across the entire test section at the end of the test was 15.9 mm (0.63 in) and 8.8 mm (0.35 in) respectively. The average maximum rut was higher than the failure criterion of 12.5 mm (0.5 in) set for the experiment, reached after approximately 1.2 million repetitions. As indicated above, testing was continued to determine whether cracking would eventually spread to the remainder of the test section. The maximum rut depth measured on the section was 30 mm (1.18 in). The rate of rutting was relatively slow during the early part of the experiment, but increased significantly after the 100 kN (22,500 lb) load change, despite the pavement temperature being reduced to $15^\circ\text{C}\pm 4^\circ\text{C}$ ($59^\circ\text{F}\pm 7^\circ\text{F}$). The final surface rutting pattern of the overlay generally corresponds with the fatigue cracking pattern, and the deepest part of the rut occurred on that half of the section with the highest density of cracking in the underlying DGAC layer.

- The two failure criteria set for the experiment were reached within approximately 300,000 load repetitions of each other.
- Ratios of final-to-initial elastic surface deflections under a 60 kN (13,500 lb) wheel load increased by between four and eleven times along the length of the section, indicating significant damage in the pavement structure in terms of loss of stiffness. The ratio of final-to-initial deflections was inconsistent across the section, with significantly higher values in the area overlying the most severely cracked area.
- Analysis of surface profiles and experience from other sections where MDD data was available, indicate that most of the permanent deformation probably occurred in the asphalt-bound surfacing layers (overlay and cracked DGAC) with approximately twice as much damage occurring in the area of most severe cracking in the underlying DGAC layer. No in-depth elastic deflection or permanent deformation data were collected in this experiment due to problems with the MDDs. Malfunction was attributed to the loss of anchorage of the modules resulting from very wet conditions in the lower layers of the pavement and subgrade.
- Parts of the test were carried out during relatively high rainfall. This resulted in ponding of water adjacent to the section. Some pumping of fines through the cracks was noted in the final days of testing.

No recommendations as to the use of the modified binders in overlay mixes are made at this time. These recommendations will be included in the second-level analysis report, which will be prepared and submitted on completion of all HVS and laboratory testing.

5. REFERENCES

1. **Generic experimental design for product/strategy evaluation — crumb rubber modified materials.** 2005. Sacramento, CA: Caltrans.
2. **Reflective Cracking Study: Workplan for the Comparison of MB, RAC-G, and DGAC Mixes Under HVS and Laboratory Testing.** 2003. Davis and Berkeley, CA: University of California Pavement Research Center. (UCPRC-WP-2003-01).
3. BEJARANO, M., Jones, D., Morton, B., and Scheffy, C. 2005. **Reflective Cracking Study: Summary of Construction Activities, Phase 1 HVS Testing, and Overlay Construction.** Davis and Berkeley, CA: University of California Pavement Research Center. (UCPRC-RR-2005-03).
4. HARVEY, J., Du Plessis, L., Long, F., Deacon, J., Guada, I., Hung, D. and Scheffy, C. 1997. **CAL/APT Program: Test Results from Accelerated Pavement Test on Pavement Structure Containing Asphalt Treated Permeable Base (ATPB) – Section 500RF.** Davis and Berkeley, CA: University of California Pavement Research Center. (Report Numbers UCPRC-RR-1999-02 and RTA-65W4845-3).
5. HARVEY, J., Du Plessis, L., Long, F., Deacon, J., Guada, I., Hung, D. and Scheffy, C. 1997. **CAL/APT Program: Test Results from Accelerated Pavement Test on Pavement Structure Containing Untreated Base – Section 501RF.** Davis and Berkeley, CA: University of California Pavement Research Center. (Report Numbers UCPRC-RR-1997-03 and RTA-65W4845-3).

